

Synthesis and Coordination Chemistry of Two N₂-Donor Chelating Di(indazolyl)methane Ligands: Structural Characterization and Comparison of Their Metal Chelation Aptitudes

Claudio Pettinari,^{*,†} Alessandro Marinelli,[†] Fabio Marchetti,[‡] Jean Ngoune,[†] Agustín Galindo,[§] Eleuterio Álvarez,^{*,§,||} and Margarita Gómez^{||}

[†]School of Pharmacy, and [‡]School of Sciences and Technologies, University of Camerino, Via S. Agostino 1, 62032 Camerino MC, Italy, [§]Departamento de Química Inorgánica, Universidad de Sevilla, Apto. 1203, 41071 Sevilla, Spain, and ^{||}Instituto de Investigaciones Químicas (IIQ), Consejo Superior de Investigaciones Científicas (CSIC), Universidad de Sevilla, Avda. Américo Vespucio 49, Isla de La Cartuja, 41092 Sevilla, Spain

Received August 4, 2010

The N₂-donor bidentate ligands di(1*H*-indazol-1-yl)methane (**L**¹) and di(2*H*-indazol-2-yl)methane (**L**²) (**L** in general) have been synthesized, and their coordination behavior toward Zn^{II}, Cd^{II}, and Hg^{II} salts has been studied. Reaction of **L**¹ and **L**² with ZnX₂ (X = Cl, Br, or I) yields [ZnX₂L] species (**1–6**), that, in the solid state, show a tetrahedral structure with dihapto ligand coordination via the pyrazolyl arms. The reaction of **L**¹ and **L**² with Zn(NO₃)₂·6H₂O is strongly dependent on the reaction conditions and on the ligand employed. Reaction of **L**¹ with equimolar quantities of Zn(NO₃)₂·6H₂O yields the neutral six-coordinate species [Zn(NO₃)₂(**L**¹)], **7**. On the other hand the use of **L**¹ excess gives the 2:1 adduct [Zn(NO₃)₂(**L**¹)₂], **8** where both nitrates act as a unidentate coordinating ligand. Analogous stoichiometry is found in the compound obtained from the reaction of **L**² with Zn(NO₃)₂·6H₂O which gives the ionic [Zn(NO₃)(**L**²)₂](NO₃), **10**. Complete displacement of both nitrates from the zinc coordination sphere is observed when the reaction between **L**¹ excess and the zinc salt was carried out in hydrothermal conditions. The metal ion type is also determining structure and stoichiometry: the reaction of **L**² with CdCl₂ gave the 2:1 adduct [CdCl₂(**L**²)₂] **11** where both chlorides complete the coordination sphere of the six-coordinate cadmium center; on the other hand from the reaction of **L**¹ with CdBr₂ the polynuclear [CdBr₂(**L**¹)]_n **12** is obtained, the Br[−] anion acting as bridging ligands in a six-coordinate cadmium coordination environment. The reaction of **L**¹ and **L**² with HgX₂ (X = Cl, I, SCN) is also dependent on the reaction conditions and the nature of X, two different types of adducts being formed [HgX(L)] (**14**: **L** = **L**¹, **16**, **17**: **L** = **L**¹ or **L**², X = I, **19**: **L** = **L**², X = SCN) and [HgX(L)₂] (**15**: **L** = **L**², X = Cl, **18**: **L** = **L**¹, X = SCN). The X-ray diffraction analyses of compounds **1**, **2**, **4**, **5**, **7**, **8**, **10–12**, **14**, **15**, and **19** are also reported. The variations of the coordination geometry parameters in the complexes are compared and discussed.

Introduction

Poly(pyrazol-1-yl)alkanes ligands were reported for the first time by Trofimenko in the early 1960s, but only in the past decade have they received increasing attention.¹ They are a family of stable and flexible bidentate ligands, isoelectronic and isosteric with the well-known bis(pyrazolyl)borates, but their coordinating behavior is often very different from that shown by the bis(pyrazolyl)borates. (R₂C)_n(pz^x)₂ ligands are able to yield stable adducts containing six M–N–N–C–N–N and seven M–N–N–C–C–N–N membered rings, basic salts, mercuriated products, cleavage of the carbon (sp³)–N bond and “agostic” interaction M···H–C between

the metal center and protons of the bridging methylene groups.^{1b} While bipy or phen metal adducts generally contain an approximately planar, five membered –M–N–C–C–N moiety, upon coordination of (R₂C)(pz^x)₂ to a metal, the six-membered cycle formed has a boat conformation. Nevertheless, both the internal and the external angles of the formally related M–(N–N)₂–C moieties are known to be able to undergo wide variations.²

Bis(pyrazolyl)alkanes offer the possibility of modulating the steric and electronic properties by introducing substituents not only in the pyrazole rings but also at the central carbon atom, and recent papers have appeared on the coordination

*To whom correspondence should be addressed. E-mail: claudio.pettinari@unicam.it. Fax: +39-0737-637345.

(1) (a) Pettinari, C.; Pettinari, R. *Coord. Chem. Rev.* **2005**, *249*, 525–543. (b) Pettinari, C.; Pettinari, R. *Coord. Chem. Rev.* **2005**, *249*, 663–691.

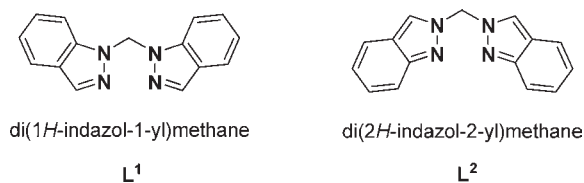
(2) (a) Canty, A. J.; Lee, C. V.; Chaichit, N.; Gatehouse, B. M. *Acta Crystallogr.* **1982**, *B38*, 743–748. (b) Lorenzotti, A.; Bovio, B.; Bonati, F.; Cingolani, A.; Gioia Lobbia, G.; Leonesi, D. *Inorg. Chim. Acta* **1990**, *170*, 199–203.

chemistry bis(pyrazolyl)methane ligands in which the central carbon atom bears phenyl rings that have different functional substituents such as OCH₃, NO₂, or NH₂.³ This field has been recently expanded by Reger, who has used bis(pyrazol-1-yl) fragments in conjunction with several bridging spacers to generate “third-generation” flexible di- and polytopic ligands able to afford complexes of several d-block metal acceptors with different nuclearity and unusual magnetic properties.⁴

The substitution of the pyrazole rings with other azoles has been another guiding motif of the past decade, triazoles and imidazoles being the most successfully employed. Our group have contributed in this field by reporting the bis(1,2,4-triazol-1-yl)alkane ligand CH₂tz₂, capable to coordinate to silver salts through the exodentate nitrogen atoms at the 4-positions of the triazole rings and yield bi- and three-dimensional polymers.⁵ We have also reported a bis(imidazol-1-yl)methane ligand able to afford novel polynuclear species based on Sn, Zn, Cd, and Hg.⁶

Although indazoles represent a widely used medicinal chemistry pharmacophore that is found on a number of marketed drugs (the indazole subunit is a frequently reported motif in drug substances with important biological activities, as for example anti-HIV activity),⁷ they have been used to a lesser extent in the synthesis of bis(azolyl)alkane-type ligands, also because of the complexity of the synthetic procedures required to prepare these ligands.⁸ Most of the reports describing

Chart 1



bis(indazolyl)methanes involve construction of tripodal system based on pyridine and containing an unsymmetrical donor set^{9a,b} or nitro-substituted indazoles.^{9c} To enlarge the bis(pyrazolyl)alkanes family, we have decided to synthesize new ligands using the indazolyl functionality,^{8b} also because this ligand family could find use in relevant biological applications.¹⁰ Here we report the synthesis and full characterization of new metal derivatives containing two of the three regioisomers depicted in Chart 1, obtained from the reactions of indazole with CH₂X₂. To our knowledge this is the first report comparing systematically the metal chelation aptitudes of different regioisomers of bis(azolyl)alkanes.¹¹

Experimental Section

General Materials and Experimental Procedures. All chemicals were purchased from Aldrich (Milwaukee, WI) and used as received. Ligands **L¹** and **L²** were prepared by following the procedure described by ref 8 and separated for the first time.^{8b} All the reactions and manipulations were performed under dry nitrogen atmosphere, and solvents were degassed prior to use; however, the reaction can also be performed in the air, but the products will invariably contain one or two water molecules, likely dispersed in the solid lattice, as observed in the crystallographic studies (see below) carried out on single crystals of one derivative, obtained from slow evaporation of chloroforms solutions performed in air. Solvent evaporations were always carried out under vacuum using a rotary evaporator. The samples for microanalysis were dried in vacuo to constant weight (20 °C, ca. 0.1 Torr). Elemental analyses (C, H, N, S) were performed in-house with a Fison Instrument 1108 CHNS-O Elemental analyzer or with a LECO-TruSpec CHN/CHNS apparatus (IIQ). IR spectra were recorded from 4000 to 200 cm⁻¹ with a Perkin-Elmer System 2000 FT-IR instrument or with Bruker Vector 22 spectrometer (IIQ). ¹H and ¹³C {¹H}NMR spectra were recorded on a 400 Mercury Plus Varian instrument operating at room temperature (400 MHz for ¹H and 100 MHz for ¹³C) or on a Bruker DRX-500 spectrometer (500 MHz for ¹H and 125 MHz for ¹³C, IIQ). H and C chemical shifts (δ) are reported in parts per million (ppm) from SiMe₄ (¹H and ¹³C calibration by internal deuterium solvent lock). Peak multiplicities are abbreviated: singlet, s; doublet, d; triplet, t; quartet, q; and multiplet, m. Electrospray mass spectra (ESIMS) were obtained using a Bruker Esquire6000 instrument (IIQ). Melting points are uncorrected and were taken on an SMP3 Stuart scientific instrument and on a capillary apparatus. The electrical conductivity measurements (Λ_M, reported as S cm² mol⁻¹) of acetonitrile and water solutions of the complexes were taken with a Crison CDTM 522 conductimeter at room temperature.

Synthesis of Di(1H-indazol-1-yl)methanezinc(II)dichloride [ZnCl₂(L¹)], **1.** To a solution of di(1H-indazol-1-yl)methane (**L¹**) (0.174 g, 0.7 mmol) in acetonitrile (10 mL), a solution of anhydrous ZnCl₂ (0.100 g, 0.7 mmol) in the same solvent (20 mL) was added. A colorless precipitate immediately formed, and the

(3) (a) Carrión, M. C.; Jalón, F. A.; Manzano, B. R.; Rodríguez, A. M.; Sepúlveda, F.; Maestro, M. *Eur. J. Inorg. Chem.* **2007**, 3961–3973. (b) Carrión, M. C.; Díaz, A.; Guerrero, A.; Jalón, F. A.; Manzano, B. R.; Rodríguez, A. *New J. Chem.* **2002**, 26, 305–312. (c) Carrión, M. C.; Sepúlveda, F.; Jalón, F. A.; Manzano, B. A.; Rodríguez, A. M. *Organometallics* **2009**, 28, 3822–3833.

(4) (a) Reger, D. L.; Foley, E. A.; Smith, M. D. *Inorg. Chem.* **2010**, 49, 234–242. (b) Reger, D. L.; Foley, E. A.; Watson, R. P.; Pellechia, P. J.; Smith, M. D.; Grandjean, F.; Long, G. J. *Inorg. Chem.* **2009**, 48, 10658–10669. (c) Reger, D. L.; Foley, E. A.; Smith, M. D. *Inorg. Chem.* **2009**, 48, 936–945. (d) Reger, D. L.; Foley, E. A.; Semeniuc, R. F.; Smith, M. D. *Inorg. Chem.* **2007**, 46, 11345–11355. (e) Reger, D. L.; Watson, R. P.; Smith, M. D.; Pellechia, P. J. *Cryst. Growth Des.* **2007**, 7, 1163–1170. (f) Reger, D. L.; Watson, R. P.; Gardinier, J. R.; Smith, M. D.; Pellechia, P. J. *Inorg. Chem.* **2006**, 45, 10088–10097. (g) Reger, D. L.; Watson, R. P.; Smith, M. D. *Inorg. Chem.* **2006**, 45, 10077–10087. (h) Reger, D. L.; Semeniuc, R. F.; Gardinier, J. R.; O’Neal, J.; Reinecke, B.; Smith, M. D. *Inorg. Chem.* **2006**, 45, 4337–4339. (i) Reger, D. L.; Watson, R. P.; Smith, M. D.; Pellechia, P. J. *Organometallics* **2006**, 25, 743–755. (j) Reger, D. L.; Watson, R. P.; Smith, M. D.; Pellechia, P. J. *Organometallics* **2005**, 24, 1544–1555. (k) Reger, D. L.; Watson, R. P.; Gardinier, J. R.; Smith, M. D. *Inorg. Chem.* **2004**, 43, 6609–6619. (l) Reger, D. L.; Brown, K. J.; Gardinier, J. R.; Smith, M. D. *Organometallics* **2003**, 22, 4973–4983.

(5) (a) Effendy, Marchetti, F.; Pettinari, C.; Pettinari, R.; Skelton, B. W.; White, A. H. *Inorg. Chem.* **2003**, 42, 112–117. (b) Effendy, Marchetti, F.; Pettinari, C.; Pettinari, R.; Ricciutelli, M.; Skelton, B. W.; White, A. H. *Inorg. Chem.* **2004**, 43, 2157–2165.

(6) (a) Masciocchi, N.; Albisetti, A. F.; Sironi, A.; Pettinari, C.; Marinelli, A. *Powder Diffraction* **2007**, 22, 236–240. (b) Masciocchi, N.; Pettinari, C.; Alberti, E.; Pettinari, R.; Di Nicola, C.; Albisetti, A. F.; Sironi, A. *Inorg. Chem.* **2007**, 46, 10491–10500. (c) Masciocchi, N.; Pettinari, C.; Alberti, E.; Pettinari, R.; Di Nicola, C.; Albisetti, A. F.; Sironi, A. *Inorg. Chem.* **2007**, 46, 10501–10509. (d) Masciocchi, N.; Albisetti, A. F.; Sironi, A.; Pettinari, C.; Di Nicola, C.; Pettinari, R. *Inorg. Chem.* **2009**, 48, 5328–5337.

(7) (a) Peruncherathan, S.; Khan, T. A.; Ila, H.; Junjappa, H. *Tetrahedron* **2004**, 60, 3457. (b) Pabba, C.; Wang, H. J.; Mulligan, S. R.; Chen, Z. J.; Stark, T. M.; Gregg, B. T. *Tetrahedron Lett.* **2005**, 46, 7553, and references therein.

(8) (a) Juliá, S.; Sala, P.; Del Mazo, J.; Sancho, M.; Ochoa, C.; Elguero, J.; Fayet, J. P.; Vertut, M. D. *J. Heterocyclic Chem.* **1982**, 19, 1141–1145. (b) Pettinari, C.; Álvarez, E.; Galindo, A. manuscript in preparation.

(9) (a) López Gallego-Preciado, M. C.; Ballesteros, P.; Claramunt, R. M.; Cano, M.; Heras, J. V.; Pinilla, E.; Monge, A. *J. Organomet. Chem.* **1993**, 450, 237–244. (b) López, M. C.; Jagerovic, N.; Ballesteros, P. *Tetrahedron: Asymmetry* **1994**, 5, 1887–1890. (c) Tabassum, S.; Parveen, S.; Arjmand, F. *Transition Met. Chem.* **2005**, 30, 196–204.

(10) (a) Schepetkin, I.; Potapov, A.; Khlebnikov, A.; Korotkova, E.; Lukina, A.; Malovichko, G.; Kirpotina, L.; Quinn, M. T. *J. Biol. Inorg. Chem.* **2006**, 11, 499–513. (b) Shiu, K.-B.; Liou, K.-S.; Wang, S.-L.; Wei, S.-C. *Organometallics* **1990**, 9, 669–675.

(11) Abbotto, A.; Bradamante, S.; Facchetti, A.; Pagani, G. A. *J. Org. Chem.* **2002**, 67, 5753–5772.

resulting suspension was stirred overnight, then filtered, and the precipitate washed with MeCN (6 mL). Recrystallization from MeCN gave colorless crystals of **1** in 60% yield. Compound **1** formed also when the reaction was carried out in EtOH. Elem. Anal. Calculated for $C_{15}H_{12}Cl_2N_4Zn$: C, 46.85; H, 3.15; N, 14.57. Found: C, 47.01; H, 3.13; N, 14.30. Mp. 297–299 °C. IR (cm^{-1}): 3105 (w), 3073 (w), 3006 (vw), 1621 (m), 1511 (m), 1466 (m), 1459 (m), 1440 (m), 1394 (w), 1362 (m), 1323 (w), 1284 (m), 1258 (m), 1224 (w), 1163 (br), 1140 (w), 1129 (w), 1051 (m), 1033 (m), 1008 (m), 972 (m), 910 (vs), 875 (w), 846 (m), 819 (ms), 776 (s), 742 (s). 1H NMR (DMSO- d_6): 7.08 (s, 2H), 7.14 (t, 2H), 7.44 (t, 2H), 7.70 (d, 2H), 7.93 (d, 2H), 8.09 (s, 2H). ESI MS (+, MeCN): 249 [100] $[H_2C(IN,IN'-ind)_2 + H]^+$, 404 [25] $[Zn\{H_2C(IN,IN'-ind)_2\}_3]^+$, 595 [26] $[ZnCl\{H_2C(IN,IN'-ind)_2\}_2]^+$. Λ_M (DMSO, 1×10^{-3} M) = 4.6 $\mu S/cm$.

Synthesis of Di(2H-indazol-2-yl)methanezinc(II)dichloride $[ZnCl_2(L^2)]$, **2.** This compound has been prepared in 65% yield, following the same procedure described for **1** by using a solution of di(2H-indazol-2-yl)methane (L^2) (0.174 g, 0.7 mmol). A colorless precipitate formed, and the resulting suspension was stirred overnight, then filtered, and the precipitate washed with MeCN (6 mL). Recrystallization from MeCN gave colorless crystals of **2**. Elem. Anal. Calculated for $C_{15}H_{12}Cl_2N_4Zn$: C, 46.85; H, 3.15; N, 14.57. Found: C, 47.10; H, 3.22; N, 14.43. Mp. 334–336 °C. IR (cm^{-1}): 3117 (w), 3014 (m), 2963 (w), 1633 (m), 1556 (w), 1522 (m), 1482 (m), 1446 (w), 1427 (m), 1361 (m), 1335 (m), 1305 (s), 1243 (m), 1196 (m), 1163 (m), 1149 (m), 1140 (m), 1128 (m), 1034 (m), 1013 (m), 987 (m), 915 (m), 848 (m), 817 (s), 766 (s), 759 (s), 695 (s). 1H NMR (DMSO- d_6): 7.00 (s, 2H), 7.03 (t, 2H), 7.22 (t, 2H), 7.55 (d, 2H), 7.73 (d, 2H), 8.70 (s, 2H). Λ_M (DMSO, 1×10^{-3} M) = 3.5 $\mu S/cm$.

Synthesis of Di(1H-indazol-2-yl)methanezinc(II)dibromide $[ZnBr_2(L^1)]$, **3.** To a solution of $ZnBr_2$ (0.100 g, 0.44 mmol) in ethanol (20 mL), di(1H-indazol-1-yl)methane (L^1) (0.250 g, 1.0 mmol) was progressively added. The milky suspension was warmed and stirred overnight. The solution was then cooled to room temperature, and a microcrystalline precipitate formed, was filtered off, and was washed twice with 3 mL of EtOH, then dried at room temperature to give **3** in 80% yield. Elem. Anal. Calculated for $C_{15}H_{12}Br_2N_4Zn$: C, 38.05; H, 2.55; N, 11.38. Found: C, 38.33; H, 2.23; N, 11.03. Mp. 280–284 °C. IR (cm^{-1}): 3113 (w), 2999 (w), 2918 (w), 1623 (m), 1510 (m), 1465 (m), 1458 (m), 1441 (w), 1394 (m), 1364 (m), 1325 (m), 1283 (m), 1260 (m), 1223 (m), 1191 (m), 1180 (m), 1155 (m), 1089 (w), 1052 (m), 1008 (w), 971 (m), 908 (m), 862 (m), 840 (m), 780 (s). 1H NMR (DMSO- d_6): δ 7.07 (s, 2H), 7.14 (t, 2H), 7.43 (t, 2H), 7.71 (d, 2H), 7.93 (d, 2H), 8.09 (s, 2H). Λ_M (DMSO, 1×10^{-3} M) = 23.9 $\mu S/cm$.

Synthesis of Di(2H-indazol-2-yl)methanezinc(II)dibromide $[ZnBr_2(L^2)]$, **4.** To a solution of $ZnBr_2$ (0.100 g, 0.44 mmol) in ethanol (20 mL), di(2H-indazol-2-yl)methane (L^2) (0.250 g, 1.0 mmol) was progressively added. The milky suspension was stirred overnight. The colorless powder was then filtered off and washed twice with 3 mL of EtOH, then dried at room temperature to give **4** in 70% yield. Elem. Anal. Calculated for $C_{15}H_{12}Br_2N_4Zn$: C, 38.05; H, 2.55; N, 11.38. Found: C, 38.53; H, 2.52; N, 11.66. Mp. 340–342 °C. IR (cm^{-1}): 3109 (w), 3009 (w), 2957 (w), 1632 (m), 1556 (w), 1521 (m), 1481 (m), 1443 (w), 1425 (m), 1360 (m), 1333 (m), 1161 (m), 1127 (s), 1031 (m), 1009 (m), 915 (s), 847 (s), 814 (s), 764 (s), 758 (s), 695 (s). 1H NMR (DMSO- d_6): δ 7.00 (s, 2H), 7.02 (t, 2H), 7.22 (t, 2H), 7.55 (d, 2H), 7.73 (d, 2H), 8.70 (s, 2H). Λ_M (DMSO, 1×10^{-3} M) = 27.7 $\mu S/cm$.

Synthesis of Di(1H-indazol-1-yl)methanezinc(II)diiodide $[ZnI_2(L^1)]$, **5.** To a solution of anhydrous ZnI_2 (0.413 g, 1.3 mmol) in acetonitrile (20 mL), L^1 (0.250 g, 1.0 mmol) was progressively added. The milky suspension was stirred overnight. The colorless powder was then filtered off and washed twice with 3 mL of CH_3CN , then dried at room temperature to give **5** in 55% yield. Elem. Anal. Calculated for $C_{15}H_{12}I_2N_4Zn$: C, 31.75; H, 2.13; N, 9.87. Found: C, 31.86; H, 2.12; N, 10.01. Mp. 110–116 °C. IR

(cm^{-1}): 3109 (w), 3009 (w), 2957 (w), 1622 (m), 1511 (w), 1463 (m), 1321 (w), 1280 (m), 1258 (m), 1224 (w), 1178 (br), 1009 (m), 968 (m), 908 (vs), 861 (w), 834 (w), 744 (br), 742 (s), 666 (w), 644 (w), 605 (w), 587 (w). 1H NMR (DMSO- d_6): δ 7.10 (s, 2H), 7.17 (t, 2H), 7.46 (t, 2H), 7.74 (d, 2H), 7.95 (d, 2H), 8.12 (s, 2H). ^{13}C NMR (DMSO- d_6): 60.67 (C1), 110.84 (C3), 121.43 (C6), 121.74 (C5), 124.46 (C8), 127.21 (C4), 134.80 (C2), 139.71 (C7). ESI MS (+): 268.6 $[ZnI(DMSO)]^+$, 346.6 $[ZnI(DMSO)_2]^+$, 438.6 $[Zn(L^1)]^+$. Λ_M (DMSO, 1×10^{-3} M) = 63.4 $\mu S/cm$.

Synthesis of Di(2H-indazol-2-yl)methanezinc(II)diiodide $[ZnI_2(L^2)]$, **6.** To a solution of anhydrous ZnI_2 (0.319 g, 1.0 mmol) in ethanol (20 mL), L^2 (0.250 g, 1.0 mmol) was progressively added. The milky suspension formed was stirred overnight. The colorless powder was then filtered off and washed twice with 3 mL of ethanol, then dried at room temperature to give **6** in 70% yield. Elem. Anal. Calculated for $C_{15}H_{12}I_2N_4Zn$: C, 31.75; H, 2.13; N, 9.87. Found: C, 31.44; H, 2.10; N, 9.81. Mp. 168–171 °C. IR (cm^{-1}): 3095 (m), 2999 (m), 2963 (w), 1626 (m), 1584 (w), 1522 (m), 1510 (m), 1477 (w), 1446 (w), 1430 (m), 1360 (m), 1336 (w), 1296 (m), 1235 (m), 1187 (m), 1161 (m), 1149 (m), 1139 (m), 1128 (m), 1083 (m), 1030 (m), 1002 (m), 978 (m), 959 (m), 918 (m), 909 (m), 861 (m), 844 (m), 820 (m), 777 (s), 759 (s), 713 (m). 1H NMR (DMSO- d_6): 7.03 (s, 2H), 7.05 (t, 2H), 7.22 (t, 2H), 7.55 (d, 2H), 7.73 (d, 2H), 8.58 (s, 2H). Λ_M (DMSO, 1×10^{-3} M) = 65.7 $\mu S/cm$.

Synthesis of Di(1H-indazol-1-yl)methanezinc(II)dinitrate $[Zn(NO_3)_2(L^1)]$, **7.** To a solution of $Zn(NO_3)_2 \cdot 6H_2O$ (0.300 g, 1.00 mmol) in MeCN (20 mL), L^1 (0.250 g, 1.0 mmol) was progressively added. The solution was stirred for 24 h at about 100 °C. Then the solution was cooled to room temperature. Colorless crystals formed that were filtered off and washed twice with 3 mL of MeCN, then dried at room temperature to give **7** in 50% yield. Elem. Anal. Calculated for $C_{15}H_{12}N_6O_6Zn$: C, 41.16; H, 2.76; N, 19.20; Found: C, 41.24; H, 2.89; N, 19.34. Mp. 239 °C. IR (cm^{-1}): 3109 (w), 3025 (w), 2973 (w), 1619 (m), 1480 (sh), 1426 (w), 1377 (m), 1314, 1300 (s,br), 1223 (m), 1175 (m), 1158 (m), 1128 (m), 1041 (m), 1015 (m), 966 (m), 908 (m), 775 (s), 752 (s), 608 (m). 1H NMR (DMSO- d_6): 7.10 (s, 2H), 7.17 (t, 2H), 7.46 (t, 2H), 7.74 (d, 2H), 7.96 (d, 2H), 8.12 (s, 2H). ^{13}C NMR (DMSO- d_6): 60.83 (C1), 110.85 (C3), 121.35 (C6), 121.81 (C5), 124.57 (C8), 127.18 (C4), 135.00 (C2), 139.75 (C7). ESI MS (+): 281.7 $[Zn(NO_3)(DMSO)]^+$, 373.7 $[Zn(NO_3)(L^1)]^+$, 621.7 $[Zn(NO_3)(L^1)_2]^+$. Λ_M (MeCN, 1×10^{-3} M) = 33.8 $\mu S/cm$.

Synthesis of Bis(di(1H-indazol-1-yl)methane)zinc(II)dinitrate $[Zn(NO_3)_2(L^1)_2]$, **8.** To a solution of $Zn(NO_3)_2 \cdot 6H_2O$ (0.300 g, 1.00 mmol) in MeCN (20 mL), L^1 (0.500 g, 2.0 mmol) was progressively added. The solution was stirred for 24 h at room temperature. Colorless crystals formed that were filtered off and washed twice with 3 mL of MeCN, then dried at room temperature to give **8** in 10% yield. From the filtered solution $[Zn(NO_3)_2(L^1)_2] \cdot 2H_2O$ was recovered in 65% yields. Elem. Anal. Calculated for $C_{30}H_{28}N_{10}O_8Zn$: C, 49.91; H, 3.91; N, 19.40; Found: C, 49.64; H, 3.89; N, 19.23. Mp. 247–250 °C. IR (cm^{-1}): 3300 (br), 3122 (w), 3063 (w), 3025 (w), 1619 (m), 1480 (sh), 1463 (m), 1416 (m), 1380 (m), 1353 (m), 1300 (s,br), 1281 (s,br), 1260 (s), 1224 (m), 1197 (m), 1175 (m), 1163 (m), 1154 (m), 1095 (w), 1031 (m), 1005 (m), 968 (w), 933 (w), 908 (m), 827 (m), 775 (m), 752 (s), 743 (sh). 1H NMR (CD_3CN): 6.99 (s, 2H), 7.27 (t, 2H), 7.58 (t, 2H), 7.79 (d, 2H), 7.94 (d, 2H), 8.20 (s, 2H). Λ_M (MeCN, 1×10^{-3} M) = 68.8 $\mu S/cm$.

Synthesis of $[Tris(di(1H-indazol-2-yl)methane)zinc(II)]dinitrate [Zn(L^1)_3](NO_3)_2$, **9.** To an acetonitrile (20 mL) solution of $Zn(NO_3)_2 \cdot 6H_2O$ (0.300 g, 1.00 mmol), L^1 (0.750 g, 3.0 mmol) was progressively added. About 5 mL of the colorless and limpid obtained solution was placed in the appropriate tube for autoclave. The sample was transferred in an autoclave, heated during 24 h at 120 °C, and then slowly cooled to room temperature at the rate of 5 °C per hour (0.083 °C min^{-1}). The complete evaporation of the solvent gives rise to a pale-orange microcrystalline powder product in 96% yield. Elem. Anal. Calculated for

Table 1. Summary of Crystallographic Data and Structure Refinement Results for **1**, **2**, **4**, **5**, **7**, **8**, and **10**

	1	2	4	5	7, 8	2(10)·H₂O
formula	C ₁₅ H ₁₂ Cl ₂ N ₄ Zn	C ₁₅ H ₁₂ Cl ₂ N ₄ Zn	C ₁₅ H ₁₂ BrN ₄ Zn	C ₁₅ H ₁₂ I ₂ N ₄ Zn	C ₆₀ H ₄₈ N ₂₂ O ₁₈ Zn ₃	C ₆₀ H ₅₀ N ₂₀ O ₁₃ Zn ₂
fw	384.56	384.56	473.48	567.46	1561.31	1389.94
crystal system	monoclinic	monoclinic	orthorhombic	monoclinic	orthorhombic	monoclinic
space group	<i>P2₁/n</i>	<i>P2₁/m</i>	<i>Pnma</i>	<i>P2₁/n</i>	<i>Pbca</i>	<i>C2/c</i>
<i>a</i> , Å	7.3100(4)	7.2900(11)	13.2080(11)	7.7578(5)	12.9233(8)	24.7270(10)
<i>b</i> , Å	13.4939(7)	14.101(2)	14.2483(12)	17.2785(10)	15.2324(9)	18.0145(6)
<i>c</i> , Å	16.1030(8)	8.2929(13)	8.5448(7)	13.1568(9)	32.563(2)	15.8766(6)
α, deg.	90	90	90	90	90	90
β, deg.	96.083(1)	112.802(4)	90	98.802(2)	90	120.4570(10)
γ, deg.	90	90	90	90	90	90
<i>V</i> , Å ³	1579.4(1)	785.9(2)	1608.1(2)	1742.8(2)	6410.1(7)	6096.3(4)
<i>Z</i> , <i>F</i> (000)	4, 776	2, 388	4, 920	4, 1064	4, 3184	4, 2856
<i>D</i> _{calc} , Mg m ⁻³	1.617	1.625	1.956	2.163	1.618	1.514
μ, mm ⁻¹	1.893	1.902	6.497	4.953	1.205	0.870
θ _{max} , deg	30.5	26.6	30.4	30.6	30.5	27.5
temp, K	173	173	173	173	173	173
no. reflns collected	39973	14539	13405	36400	152099	74587
no. reflns used	4828	1686	2524	5317	9800	6858
no. of param.	199	106	106	199	466	433
R ₁ (<i>F</i>) [<i>F</i> ² > 2σ(<i>F</i> ²)] ^a	0.025	0.050	0.038	0.036	0.042	0.030
wR ₂ (<i>F</i> ²) ^b (all data)	0.068	0.186	0.097	0.094	0.117	0.084
S ^c (all data)	1.034	1.044	1.038	1.122	1.078	1.056

^a R₁(*F*) = ∑||*F*_o| - |*F*_c||/∑|*F*_o| for the observed reflections [*F*² > 2σ(*F*²)]. ^b wR₂(*F*²) = {∑w(*F*_o² - *F*_c²)/∑w(*F*_o²)^{1/2}}. ^c S = {∑[w(*F*_o² - *F*_c²)]/(*n* - *p*)^{1/2}}; (*n* = number of reflections, *p* = number of parameters).

C₄₅H₃₆N₁₄O₆Zn: C, 57.85; H, 3.88; N, 20.99. Found: C, 57.75; H, 4.29; N, 20.96. IR (cm⁻¹): 3108 (vw), 3062 (vw), 1657 (w), 1617 (m), 1498 (m), 1463 (s), 1439 (m), 1416 (s), 1353 (s), 1303 (br), 1279 (s), 1196 (s), 1164 (m), 1149 (m), 1097(w), 1025 (vw), 1005 (s), 934 (s), 907 (s), 827 (s), 757 (s), 736 (s). ¹H NMR (CD₃CN): 6.97 (s, 6H), 7.20 (t, 6H), 7.49 (t, 2H), 7.77 (d, 6H), 7.81 (d, 6H), 8.04 (s, 6H). Λ_M (DMSO, 1 × 10⁻³ M) = 71.2 μS/cm.

Synthesis of Bis(di(2*H*-indazol-2-yl)methane)zinc(II)dinitrate [**Zn(NO₃)(L²)₂(NO₃)·1/2H₂O**, **10**]. To a solution of Zn(NO₃)₂·6H₂O (0.300 g, 1.00 mmol) in MeCN (20 mL), L² (0.500 g, 2.0 mmol) was progressively added. The solution was stirred overnight at about 80 °C. Then the solution was cooled to room temperature. Colorless crystals formed that were filtered off and washed twice with 3 mL of MeCN, then dried at room temperature to give **10** in 50% yield. Elem. Anal. Calculated for C₃₀H₂₅N₁₀O_{6.5}Zn: C, 51.85; H, 3.63; N, 20.15; Found: C, 51.63; H, 3.44; N, 19.96. Mp. 237–239 °C. IR (cm⁻¹): 3300(w), 3109 (w), 3025 (w), 2973 (w), 1632 (m), 1556 (w), 1519 (m), 1474 (s), 1426 (w), 1376 (m), 1333 (s), 1328 (s), 1301 (s), 1280 (s), 1241 (m), 1195 (w), 1160 (m), 1127 (s), 1027 (m), 1006 (m), 987 (m), 913 (s), 844 (s), 827 (m), 812 (m), 764 (s), 758 (s), 745 (s), 692 (m). ¹H NMR (CD₃CN): 7.0 (s, 6H), 7.31 (s, 2H), 7.79 (d, 2H), 8.81 (s, 2H). ¹³C NMR (CD₃CN): 66.86 (C1), 116.1 (C3), 122.23 (C6), 122.55 (C8), 123.97 (C5), 125.57 (C2), 130.02 (C4), 149.49 (C7). Λ_M (MeCN, 1 × 10⁻³ M) = 62.8 μS/cm.

Synthesis of Bis(di(2*H*-indazol-2-yl)methane)cadmium(II)chloride [**CdCl₂(L²)₂**, **11**]. This compound has been prepared in 95% yield following the same procedure described for **3** by using an ethanol solution of L² (0.174 g, 0.7 mmol) and CdCl₂ (0.064 g, 0.35 mmol). Recrystallization from EtOH gave colorless crystals of **11**. Elem. Anal. Calculated for C₃₀H₂₄CdCl₂N₈: C, 53.00; H, 3.56; N, 16.48. Found: C, 53.22; H, 3.72; N, 16.30. Mp. 338–340 °C. IR (cm⁻¹): 3111 (w), 2986 (w), 1632 (m), 1519 (m), 1478 (m), 1446 (w), 1423 (w), 1390 (w), 1371 (w), 1333 (w), 1309 (m), 1300 (m), 1241 (w), 1162 (m), 1144 (m), 1127 (w), 1007 (m), 982 (w), 912 (m), 840 (m), 811 (m), 754 (s), 741 (s), 692 (s). ¹H NMR (DMSO-*d*₆): 7.03 (t, 2H), 7.07 (s, 2H), 7.25 (t, 2H), 7.58 (d, 2H), 7.75 (d, 2H), 8.71 (s, 2H). Λ_M (DMSO, 1 × 10⁻³ M) = 11.9 μS/cm.

Synthesis of Polymeric [(Di(1*H*-indazol-1-yl)methane)cadmium(II)bromide] [CdBr₂(L¹)_n, **12**. This compound has been prepared in 92% yield following the same procedure described for **3** by using an ethanol solution of L¹ (0.250 g, 1.0 mmol) and CdBr₂·4H₂O (0.344 g, 1.0 mmol). Recrystallization from EtOH gave colorless

crystals of **12**. Elem. Anal. Calculated for C₁₅H₁₂Br₂CdN₄: C, 34.61; H, 2.32; N, 10.76. Found: C, 34.48; H, 2.18; N, 10.54. Mp. 283–285 °C. IR (cm⁻¹): 3109 (w), 3057 (w), 2993 (w), 2951 (w), 1620 (m), 1506 (m), 1464 (m), 1455 (m), 1420 (m), 1378 (m), 1317 (w), 1284 (m), 1262 (m), 1220 (m), 1193 (m), 1170 (m), 1155 (sh), 1034 (w), 984 (w), 959 (m), 906 (m), 871 (m), 852 (w), 839 (m), 768 (s), 735 (s). ¹H NMR (CD₃CN): 7.02 (s, 2H), 7.21 (t, 2H), 7.54 (t, 2H), 7.76 (d, 2H), 7.91 (d, 2H), 8.14 (s, 2H).

Synthesis of Bis(di(1*H*-indazol-1-yl)methane)cadmium(II)nitrato [**Cd(NO₃)₂(L¹)₂**, **13**]. This compound has been prepared following the same procedure described for **3** by using an acetonitrile solution of L¹ (0.250 g, 1.0 mmol) and Cd(NO₃)₂·4H₂O (0.337 g, 1.0 mmol). The solution was stirred overnight at room temperature. Colorless powder formed upon slow evaporation, that was filtered off and washed twice with 3 mL of MeCN, then dried at room temperature to give **13** in 65% yield. Elem. Anal. Calculated for C₃₀H₂₄N₁₀O₆Cd: C, 49.16; H, 3.30; N, 19.11; Found: C, 49.23; H, 3.50; N, 19.00. Mp. 256–258 °C. IR (cm⁻¹): 3109 (w), 3015 (w), 1508 (w), 1458 (s), 1433 (s), 1301 (s), 1283 (s), 1220 (m), 1194 (w), 1172 (m), 1159 (w), 1131 (w), 1038 (m), 1008 (m), 958 (m), 909 (m), 862 (m), 833 (m), 777 (m), 768 (m), 745 (m). ¹H NMR (CD₃CN): 7.0 (s, 2H), 7.23 (t, 2H), 7.56 (t, 2H), 7.80 (d, 2H), 7.94 (d, 2H), 8.18 (s, 2H). Λ_M (MeCN, 1 × 10⁻³ M) = 31.6 μS/cm.

Synthesis of Di(1*H*-indazol-1-yl)methanemercurydichloride [**HgCl₂(L¹)₂**, **14**]. To a solution of HgCl₂ (0.054 g, 0.2 mmol) in MeCN (4 mL), L¹ (0.100 g, 0.4 mmol) was progressively added. The sample was transferred in an autoclave and was heated during 18 h at 120 °C. The solution was then cooled to room temperature, and a microcrystalline precipitate formed that was filtered off and washed twice with 3 mL of MeCN, then dried at room temperature to give **14** in 82% yield. Elem. Anal. Calculated for C₁₅H₁₂Cl₂HgN₄: C, 34.66; H, 2.33; N, 10.78. Found: C, 34.83; H, 2.25; N, 10.77. Mp. 188–190 °C. IR (cm⁻¹): 3105 (w), 3060 (w), 3008 (w), 2959 (w), 1616 (w), 1514 (m), 1465 (m), 1446 (m), 1432 (w), 1382 (m), 1374 (m), 1316 (m), 1280 (s), 1260 (m), 1216 (m), 1194 (m), 1166 (s), 1116 (m), 1033 (m), 1004 (m), 946 (m), 905 (m), 860 (m), 767 (m), 750 (s), 739 (s). ¹H NMR (CDCl₃): 6.99 (s, 2H), 7.18 (t, 2H), 7.45 (t, 2H), 7.69 (d, 2H), 7.73 (d, 2H), 8.07 (s, 2H). ¹H NMR (CD₃CN): 6.99 (s, 2H), 7.18 (t, 2H), 7.49 (t, 2H), 7.73 (d, 2H), 7.88 (d, 2H), 8.03 (s, 2H). ¹H NMR (DMSO-*d*₆): 7.10 (s, 2H), 7.17 (t, 2H), 7.46 (t, 2H), 7.74 (d, 2H), 7.96 (d, 2H), 8.12 (s, 2H). ¹³C NMR (DMSO-*d*₆): 60.58 (C1), 110.78 (C3), 121.41 (C6), 121.69 (C5), 124.47 (C8), 127.19

Table 2. Summary of Crystallographic Data and Structure Refinement Results for **11**, **12**, **14**, **15**, and **19**

	11	12	14	15	19
formula	C ₃₀ H ₂₄ CdCl ₂ N ₈	C ₁₅ H ₁₂ Br ₂ CdN ₄	C ₁₅ H ₁₂ Cl ₂ HgN ₄	C ₃₀ H ₂₄ Cl ₂ HgN ₈	C ₁₇ H ₁₂ HgN ₆ S ₂
fw	679.87	520.51	519.78	768.06	565.04
crystal system	triclinic	monoclinic	triclinic	monoclinic	monoclinic
space group	<i>P1</i>	<i>C2/c</i>	<i>P1</i>	<i>C2</i>	<i>P2₁/n</i>
<i>a</i> , Å	7.9331(12)	14.2328(8)	11.3692(6)	13.7287(8)	12.3387(5)
<i>b</i> , Å	7.9480(12)	17.1136(8)	11.6571(6)	8.4876(6)	8.1098(3)
<i>c</i> , Å	12.5068(18)	14.7971(12)	12.2672(7)	25.2150(19)	18.1621(7)
α, deg.	83.519(7)	90	95.651(2)	90	90
β, deg.	72.527(7)	117.485(2)	93.150(2)	104.348(2)	96.9590(10)
γ, deg.	67.587(6)	90	98.333(2)	90	90
<i>V</i> , Å ³	695.37(18)	3197.4(3)	1596.85(15)	2846.5(3)	2041.6(5)
<i>Z</i>	1, 342	8, 1984	4, 976	4, 1496	4, 1072
<i>D</i> _{calc} , Mg m ⁻³	1.624	2.163	2.162	1.792	2.080
μ, mm ⁻¹	1.014	6.365	9.973	5.631	8.777
θ _{max} , deg	30.4	30.9	30.6	30.4	30.5
temp, K	173	173	173	173	173
no. reflns collected	12556	52607	61132	56235	36570
no. reflns used	4932	4965	9710	8187	5310
no. of param.	371	199	397	374	235
R ₁ (<i>F</i>) [<i>F</i> ² > 2σ(<i>F</i> ²)] ^a	0.066	0.038	0.046	0.066	0.035
wR ₂ (<i>F</i> ²) ^b (all data)	0.187	0.119	0.131	0.196	0.096
S ^c (all data)	1.080	1.058	1.078	1.139	1.073

^a R₁(*F*) = ∑||*F*_o| - |*F*_c||/∑|*F*_o| for the observed reflections [*F*² > 2σ(*F*²)]. ^b wR₂(*F*²) = {∑w(*F*_o² - *F*_c²)²/∑w(*F*_o²)²}^{1/2}. ^c S = {∑[w(*F*_o² - *F*_c²)]/(*n* - *p*)^{1/2}; (*n* = number of reflections, *p* = number of parameters).

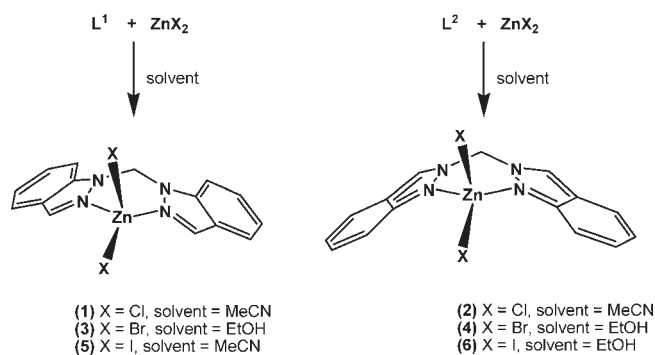
(C4), 134.82 (C2), 139.73 (C7). ESI MS (+): 271.0 [(L¹) + Na⁺]⁺, 519.1 [Hg(Cl₂)(L¹)]⁺. Λ_M (DMSO, 1 × 10⁻³ M) = 0.3 μS/cm.

Synthesis of Bis(di(2*H*-indazol-2-yl)methane)mercurydichloride [HgCl₂(L²)₂], **15.** This compound has been prepared in 40% yield following the same procedure described for **3** by using an ethanol solution of L² (0.500 g, 2.0 mmol) and HgCl₂ (0.271 g, 1.00 mmol). A colorless precipitate formed, and the resulting suspension was stirred overnight, then filtered and the precipitate washed with MeCN (6 mL). The same product afforded when the reaction between L² and HgCl₂ was carried out in MeCN during 18 h at 120 °C. Elem. Anal. Calculated for C₃₀H₂₄Cl₂HgN₈: C, 46.91; H, 3.15; N, 14.59. Found: C, 46.84; H, 3.02; N, 14.43. Mp. 180–187 °C. IR (cm⁻¹): 3116 (m), 3062 (w), 3008 (m), 2964 (w), 1630 (m), 1516 (m), 1473 (m), 1440 (w), 1417 (w), 1389 (m), 1365 (m), 1332 (m), 1298 (s), 1238 (m), 1158 (s), 1140 (m), 1125 (m), 999 (m), 979 (m), 909 (m), 838 (m), 799 (s), 752 (m), 726 (s), 693 (m). ¹H NMR (CD₃CN): 6.98 (s, 2H), 7.12 (t, 2H), 7.33 (t, 2H), 7.67 (d, 2H), 7.75 (d, 2H), 8.50 (s, 2H). ¹H NMR (DMSO-*d*₆): 7.05 (t, 2H), 7.08 (s, 2H), 7.26 (t, 2H), 7.59 (d, 2H), 7.75 (d, 2H), 8.72 (s, 2H). ¹³C NMR (DMSO-*d*₆): 67.93 (C1), 117.76 (C3), 121.52 (C6), 121.88 (C8), 122.21 (C5), 125.57 (C2), 126.91 (C4), 149.25 (C7). ESI MS (+): 270.9 [(L²) + Na⁺]⁺, 518.8 [Hg(Cl₂)(L²)]⁺, 807.0 [Hg(Cl₂)(L²)₂ + K⁺]⁺. Λ_M (DMSO, 1 × 10⁻³ M) = 4.5 μS/cm.

Synthesis of Di(1*H*-indazol-1-yl)methane)mercurydiiodide [HgI₂(L¹)], **16.** This compound has been prepared in 55% yield following the same procedure described for **3** by using an ethanol solution of L¹ (0.500 g, 2.0 mmol) and HgI₂ (0.454 g, 1.0 mmol). A colorless precipitate formed, and the resulting suspension was stirred overnight, then filtered and the precipitate washed with EtOH (6 mL) and identified as **16**. Elem. Anal. Calculated for C₁₅H₁₂HgI₂N₄: C, 25.64; H, 1.72; N, 7.97. Found: C, 25.82; H, 1.59; N, 7.87. Mp. 180–182 °C. IR (cm⁻¹): 3113 (w), 3097 (w), 3058 (w), 2956 (w), 1617 (m), 1502 (m), 1462 (m), 1421 (m), 1360 (m), 1279 (s), 1255 (m), 1218 (m), 1194 (w), 1161 (s br), 1027 (m), 1004 (w), 947 (m), 904 (s), 860 (s), 839 (s), 765 (s), 737 (s). ¹H NMR (CDCl₃): 6.93 (s, 2H), 7.20 (t, 2H), 7.39 (t, 2H), 7.68 (d, 2H), 7.83 (d, 2H), 8.03 (s, 2H). ¹H NMR (CD₃CN): 6.96 (s, 2H), 7.20 (t, 2H), 7.44 (t, 2H), 7.82 (d, 2H), 7.89 (d, 2H), 8.04 (s, 2H). Λ_M (DMSO, 1 × 10⁻³ M) = 0.4 μS/cm.

Synthesis of Di(2*H*-indazol-2-yl)methane)mercurydiiodide [HgI₂(L²)], **17.** This compound has been prepared in 65% yield following the same procedure described for **3** by using an ethanol

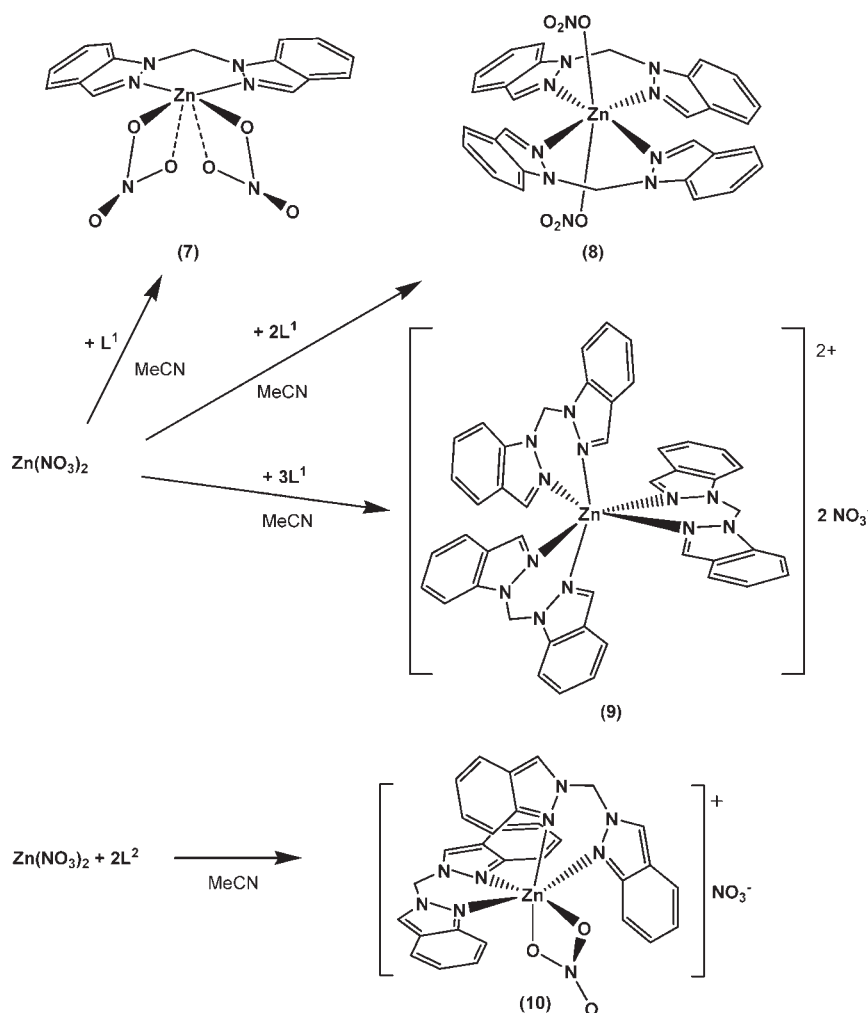
Scheme 1



solution of L² (0.500 g, 2.0 mmol) and HgI₂ (0.454 g, 1.0 mmol). A colorless precipitate formed and the resulting suspension was stirred overnight, then filtered and the precipitate washed with EtOH (6 mL) and identified as **17**. Elem. Anal. Calculated for C₁₅H₁₂HgI₂N₄: C, 25.64; H, 1.72; N, 7.97. Found: C, 25.67; H, 1.61; N, 7.74. Mp. 229–231 °C. IR (cm⁻¹): 3113 (m), 2998 (m), 1630 (m), 1517 (m), 1471 (m), 1436 (w), 1417 (w), 1390 (w), 1356 (w), 1325 (w), 1298 (s), 1301 (s), 1240 (m), 1143 (m), 1136 (s), 998 (m), 982 (m), 909 (m), 838 (m), 799 (s), 753 (m), 726 (s), 688 (m). ¹H NMR (CDCl₃): 6.93 (s, 2H), 7.26 (t, 2H), 7.31 (t, 2H), 7.62 (d, 2H), 7.75 (d, 2H), 8.27 (s, 2H). Λ_M (DMSO, 1 × 10⁻³ M) = 0.3 μS/cm.

Synthesis of Bis(di(1*H*-indazol-1-yl)methane)mercurydithiocyanate [Hg(SCN)₂(L¹)₂], **18.** This compound has been prepared in 55% yield following the same procedure described for **9** by using an acetonitrile solution of L¹ (0.500 g, 2.0 mmol) and Hg(SCN)₂ (0.316 g, 1.0 mmol). About 3 mL of the colorless and limpid obtained solution was placed in the appropriate tube for autoclave. The sample transferred in an autoclave, was heated during 24 h at 120 °C, then slowly cooled to room temperature at the rate of 5 °C per hour (0.083 °C min⁻¹). The complete evaporation of the solvent gives rise to a colorless microcrystalline powder, recrystallized from MeCN and identified as **18**. Elem. Anal. Calculated for C₃₄H₂₄HgN₁₀S₂: C, 47.26; H, 2.97; N, 17.22; S, 7.88. Found: C, 46.46; H, 2.91; N, 17.04; S, 8.18. Mp. 160–162 °C. IR (cm⁻¹): 3103 (w), 3063 (w), 2958 (w), 2918 (w), 2849 (w), 1618 (w), 1617 (m), 1500 (w), 1464 (m), 1439 (w), 1417

Scheme 2



(m), 1354 (m), 1304 (w), 1280 (m), 1197 (br), 1164 (m), 1098 (w), 1025 (vw), 1005 (w), 935 (m), 907 (s), 828 (m), 758 (m), 735 (br). $^1\text{H NMR}$ (CD_3CN): 6.92 (s, 2H), 7.20 (t, 2H), 7.46 (t, 2H), 7.75 (d, 2H), 7.89 (d, 2H), 8.04 (s, 2H). $^1\text{H NMR}$ ($\text{DMSO}-d_6$): 7.08 (s, 2H), 7.12 (t, 2H), 7.43 (t, 2H), 7.71 (d, 2H), 7.94 (d, 2H), 8.09 (s, 2H). Λ_M (DMSO , $1 \times 10^{-3} \text{ M}$) = $3.5 \mu\text{S}/\text{cm}$.

Synthesis of (Di(2*H*-indazol-2-yl)methane)mercuridithiocyanate [$\text{Hg}(\text{SCN})_2(\text{L}^2)$], **19.** This compound has been prepared in 72% yield following the same procedure described for **3** by using an acetonitrile solution of L^2 (0.500 g, 2.0 mmol) and $\text{Hg}(\text{SCN})_2$ (0.316 g, 1.0 mmol). A colorless precipitate formed, and the resulting suspension was stirred overnight, then filtered and the precipitate **19**, washed with EtOH (6 mL). Elem. Anal. Calculated for $\text{C}_{17}\text{H}_{12}\text{HgN}_6\text{S}_2$: C, 36.14; H, 2.14; N, 14.87; S, 11.35. Found: C, 36.18; H, 2.04; N, 14.48; S, 11.66. Mp. 173–175°C. IR (cm^{-1}): 3136 (w), 3121 (w), 3078 (w), 2126 (s), 1630 (m), 1518 (m), 1471 (m), 1305 (m), 1292 (m), 1241 (m), 1160 (m), 1126 (m), 1013 (m), 981 (m), 911 (m), 843 (m), 816 (s), 804 (s), 756 (s), 694 (m). $^1\text{H NMR}$ (CD_3CN): 6.99 (s, 2H), 7.15 (t, 2H), 7.36 (t, 2H), 7.72 (d, 2H), 7.78 (d, 2H), 8.55 (s, 2H). Λ_M (DMSO , $1 \times 10^{-3} \text{ M}$) = $2.3 \mu\text{S}/\text{cm}$.

Computational Details. The electronic structure and geometries of the model compounds were computed within the density functional theory (DFT) at the B3LYP level^{12,13} using the 6-311G* basis set for all the atoms. All the optimized geometries were characterized as local energy minima by diagonalization of the analytically computed Hessian (vibrational frequencies

calculations). The DFT calculations were performed using the Gaussian 03 suite of programs.¹⁴ Cartesian coordinates for the optimized molecules are included as Supporting Information.

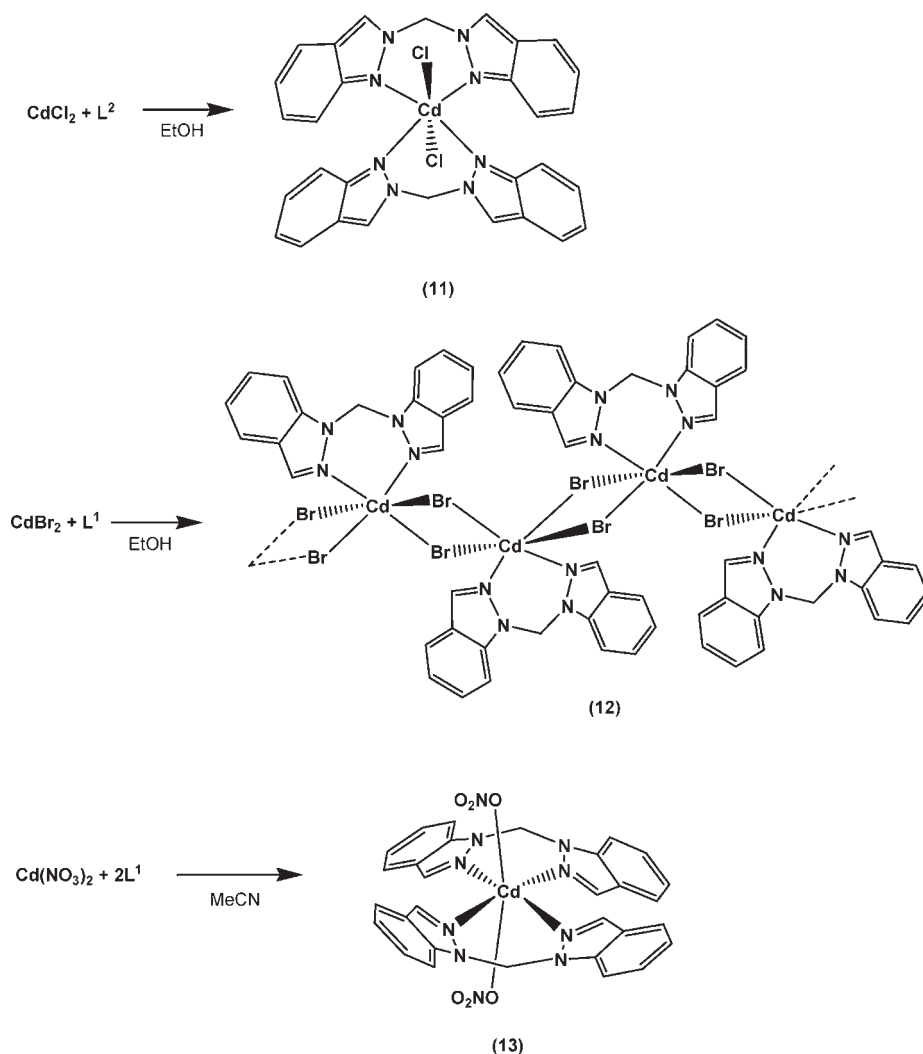
Crystallographic Structure Determinations. A summary of crystallographic data and structure refinement results for **1**, **2**, **4**, **5**, **7**, **8**, and **10** is given in Table 1, and for **11**, **12**, **14**, **15**, and **19** in Table 2. A single crystal of suitable size, obtained as indicated above, coated with dry perfluoropolyether was mounted on a glass fiber and fixed in a cold nitrogen stream [$T = 173(2) \text{ K}$] to the goniometer head. Data collection was performed on Bruker-Nonius X8APEX-II CCD diffractometer, using monochromatic radiation λ ($\text{Mo K}\alpha_1$) = 0.71073 \AA , by means of ω and

(12) Becke, A. D. *J. Chem. Phys.* **1993**, *98*, 5648.

(13) Lee, C.; Yang, W.; Parr, R. G. *Phys. Rev. B.* **1988**, *37*, 785.

(14) Frisch, M. J.; Trucks, G. W.; Schlegel, H. B.; Scuseria, G. E.; Robb, M. A.; Cheeseman, J. R.; Montgomery, J. A., Jr.; Vreven, T.; Kudin, K. N.; Burant, J. C.; Millam, J. M.; Iyengar, S. S.; Tomasi, J.; Barone, V.; Mennucci, B.; Cossi, M.; Scalmani, G.; Rega, N.; Petersson, G. A.; Nakatsuji, H.; Hada, M.; Ehara, M.; Toyota, K.; Fukuda, R.; Hasegawa, J.; Ishida, M.; Nakajima, T.; Honda, Y.; Kitao, O.; Nakai, H.; Klene, M.; Li, X.; Knox, J. E.; Hratchian, H. P.; Cross, J. B.; Bakken, V.; Adamo, C.; Jaramillo, J.; Gomperts, R.; Stratmann, R. E.; Yazyev, O.; Austin, A. J.; Cammi, R.; Pomelli, C.; Ochterski, J. W.; Ayala, P. Y.; Morokuma, K.; Voth, G. A.; Salvador, P.; Dannenberg, J. J.; Zakrzewski, V. G.; Dapprich, S.; Daniels, A. D.; Strain, M. C.; Farkas, O.; Malick, D. K.; Rabuck, A. D.; Raghavachari, K.; Foresman, J. B.; Ortiz, J. V.; Cui, Q.; Baboul, A. G.; Clifford, S.; Cioslowski, J.; Stefanov, B. B.; Liu, G.; Liashenko, A.; Piskorz, P.; Komaromi, I.; Martin, R. L.; Fox, D. J.; Keith, T.; M. A. Al-Laham, Peng, C. Y.; Nanayakkara, A.; Challacombe, M.; Gill, P. M. W.; Johnson, B.; Chen, W.; Wong, M. W.; Gonzalez, C.; Pople, J. A. *Gaussian 03*, Revision C.02; Gaussian, Inc.: Wallingford, CT, 2004.

Scheme 3



φ scans. The data were reduced (SAINT)¹⁵ and corrected for Lorentz polarization effects and absorption by the multiscan method applied by SADABS.¹⁶ The structure was solved by direct methods (SIR-2002)¹⁷ and refined against all F^2 data by full-matrix least-squares techniques (SHELXTL-6.12).¹⁸ All the non-hydrogen atoms were refined with anisotropic displacement parameters. The hydrogen atoms were included from calculated positions and refined riding on their respective carbon atoms with isotropic displacement parameters.

Results and Discussion

Syntheses and Characterization of Di(indazolyl)methane Complexes. Zn^{II} is a metal ion with one of the highest affinities for bis(azolyl)alkanes^{19a} and tends to form tetrahedral complexes with such ligands. Accordingly, reaction of 1 equiv of L^1 or L^2 with ZnX_2 ($\text{X} = \text{Cl}, \text{Br}, \text{or I}$) in

methanol or acetonitrile proceeds readily at room temperature to give $[\text{ZnX}_2(\text{L})]$ complexes **1–6** (Scheme 1).

Compounds **1–6** are poorly soluble in MeOH and MeCN, moderately soluble in dimethylsulfoxide (DMSO) and dimethylformamide (DMF), and insoluble in chlorinate solvents.

The reaction of (Scheme 2) with $\text{Zn}(\text{NO}_3)_2 \cdot 6\text{H}_2\text{O}$ is dependent L^1 on the ligand to metal ratio employed. In excess of the N_2 -donor ligand, the 2:1 and 3:1 adducts afforded $[\text{Zn}(\text{NO}_3)_2(\text{L}^1)_2]$ **8** and $[\text{Zn}(\text{L}^1)_3](\text{NO}_3)_2$ **9**, whereas when the reaction was carried out in strictly equimolar conditions, the 1:1 adduct $[\text{Zn}(\text{NO}_3)_2(\text{L}^1)]$ **7** is produced. On the other hand when L^2 and $\text{Zn}(\text{NO}_3)_2 \cdot 6\text{H}_2\text{O}$ were reacted, the 2:1 adduct $[\text{Zn}(\text{NO}_3)_2(\text{L}^2)_2][\text{NO}_3]^-$ **10** has been always the only product isolated (Scheme 2).

L^2 reacts with CdCl_2 giving the 2:1 adduct $[\text{CdCl}_2(\text{L}^2)_2]$ **11** also when the reaction is carried out in equimolar quantities, whereas from the reaction between L^1 and CdBr_2 , the polynuclear $[\text{CdBr}_2(\text{L}^1)]_n$ **12** is obtained (Scheme 3). No adduct afforded in the same condition by reacting L^2 with CdBr_2 . Cadmium is highly toxic to humans, animals, and plants. It has partly similar properties as zinc, so we have tried to verify if our ligands selectively coordinate cadmium or zinc. In the same reaction flask we have added equimolar quantities of ZnBr_2 , CdBr_2 , and L^1 . On the basis of

(15) SAINT, 6.02; BRUKER-AXS, Inc.: Madison, WI, 1997–1999.

(16) Sheldrick, G. SADABS; Bruker AXS, Inc.: Madison, WI, 1999.

(17) SIR2002; Burla, M. C.; Camalli, M.; Carrozzini, B.; Cascarano, G.L.; Giacovazzo, C.; Polidori, G.; Spagna, R. *J. Appl. Crystallogr.*, **2003**, *36*, 1103.

(18) SHELXTL, 6.14; Bruker AXS, Inc.: Madison, WI, 2000–2003.

(19) (a) Pettinari, C.; Marchetti, F.; Cingolani, A.; Leonesi, D.; Colapietro, M.; Margadonna, S. *Polyhedron* **1998**, *17*, 4145–4154, and references therein. (b) Aposhian, H. V.; Maiorino, R. M.; Gonzalez-Ramirez, D.; Zuniga-Charles, M.; Xu, Z.; Hurlbut, K. M.; Junco-Munoz, P.; Dart, R. C.; Aposhian, M. M. *Toxicology* **1995**, *97*, 23–38. (c) Campbell, J. R.; Clarkson, T. W.; Omar, M. D. *J. Am. Med. Assoc.* **1986**, *256*, 3127–3130.

thermogravimetric analysis (TGA), IR, and elemental analysis, we have found the formation of **3** and **12** in the molar ratio of 1 to 9. $[\text{Cd}(\text{NO}_3)_2(\text{L}^1)_2]$ **13** has been prepared analogously to **8**, and on the basis of analytical and spectral data we hypothesize for it an analogous structure.

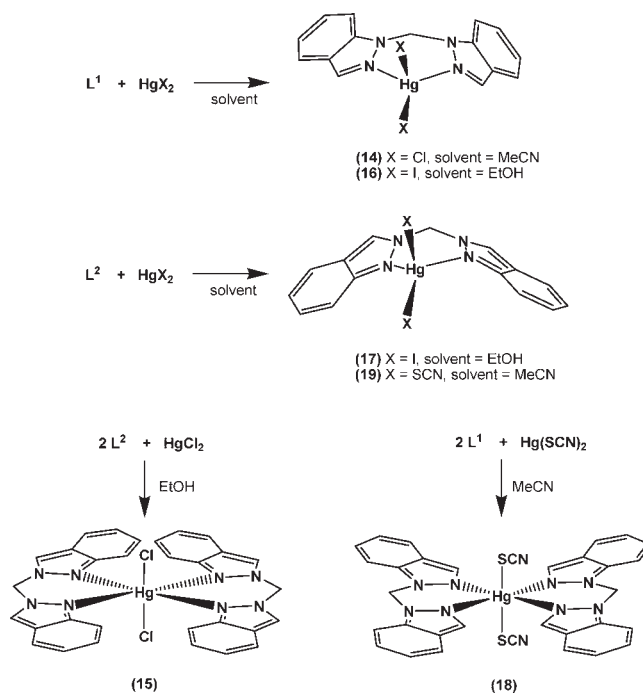
Chelating agents are used to detoxify poisonous metal agents such as mercury, arsenic, and lead by converting them to a chemically inert form that can be excreted without further interaction with the body. Despite the large clinical use of the chelation therapy to remove mercury, none of the drugs currently in use have been shown to chelate mercury, most of the structural criteria for the optimal binding of Hg^{2+} being not well elucidated.^{19b,c} For this reason we have investigated the chelating ability of L^1 and L^2 also toward a series of HgX_2 acceptors. The reaction between L^1 and HgX_2 ($\text{X} = \text{Cl}$ or I) produced tetrahedral 1:1 adducts $[\text{HgX}_2(\text{L}^1)]$ (**14**: $\text{X} = \text{Cl}$; **16**: $\text{X} = \text{I}$), as also the reaction between L^2 and HgCl_2 or $\text{Hg}(\text{SCN})_2$, the complexes $[\text{HgI}_2(\text{L}^2)]$ **17** and $[\text{Hg}(\text{SCN})_2(\text{L}^2)]$ **19** being, respectively, obtained. On the other hand the reactions between L^2 and HgCl_2 and L^1 with $\text{Hg}(\text{SCN})_2$ afforded the 2:1 complexes $[\text{HgCl}_2(\text{L}^2)_2]$ **15** and $[\text{Hg}(\text{SCN})_2(\text{L}^1)_2]$ **18** (Scheme 4).

The IR spectra of all complexes show a slight displacement to higher wavenumbers (Supporting Information, Table S1) of the $\nu(\text{C}=\text{C})$ and $\nu(\text{C}=\text{N})$ frequency compared to that of the corresponding free ligands L^1 and L^2 (Supporting Information, Figure S1), for example, from 1615 to 1628 and from 1498 to 1511 cm^{-1} in **1**, and from 1628 to 1633 and from 1515 to 1522 cm^{-1} in **2**, respectively. Moreover, strong absorption bands at about 640 and 610 cm^{-1} have been assigned to ring deformation modes.^{20,21} It is interesting that for both L^1 and L^2 complexes the displacement is greater in zinc with respect to cadmium complexes and negligible in mercury species.

In the IR spectra of the nitrate derivatives straightforward assignments of the two highest frequency bands ν_1 and ν_3 of NO_3 groups are not possible because of the presence of many overlapped ligand bands in the region 1600–1200 cm^{-1} . However in the overtone region several weak bands at 1700–1800 cm^{-1} due to $\nu_1 + \nu_4$ combination bands have been detected which can help in distinguishing ionic or coordinate nitrates.^{22,23} A bidentate coordinate nitrate is present in **7** where the splitting of $\nu_1 + \nu_4$ combination bands is about 50 cm^{-1} . Derivative **8** exhibits two weak bands, the splitting Δ being about 30 cm^{-1} in accordance with an unidentate nitrate group in the solid state, whereas in the spectrum of derivative **10** three weak absorptions have been detected in the same region, indicative of the existence of both ionic and coordinate nitrate groups. This compound likely contains a six-coordinate metal atom surrounded by four nitrogen atoms and two oxygen atoms. In **9** the ν_2 at about 827 and the ν_3 at about 1463 cm^{-1} are in accordance with the presence ionic nitrate groups.²⁴

The most significant information from the infrared spectra of compounds **18** and **19** is related to the frequency of the absorption band due to the stretching vibration of

Scheme 4



($\text{SC}\equiv\text{N}$); this band was reported to be sensitive to the bonding type of the NCS group in metal complexes.^{25,26} In the spectra of **18** and **19**, this band is high-frequency shifted, at 2126 cm^{-1} , which is suggestive of a $\text{Hg}-\text{SCN}$ bond.^{25,26}

In the ^1H NMR spectra, recorded for **1**–**19** in CDCl_3 , CD_3CN , or $\text{DMSO}-d_6$ (the choice was dictated by the solubility), most of the signals are slightly displaced toward lower field upon coordination (see Experimental Section and Supporting Information, Table S2), as already seen in the zinc, cadmium, or mercury derivatives of similar N_2 -donor ligands.^{27–31} The observed downfield shift in **8**, **10**, **13**, and **19** is additional evidence in favor of the existence, at least partial, of the complexes in that solvent. The shift generally decreases with decreasing concentration of the sample. In DMSO the displacement of the proton and carbon signals on going from the free to the bonded ligand in the adduct is negligible, in accordance with an extensive solvation and complete ligand dissociation in strongly coordinating solvents.

The ESI mass spectra of **1**, **5**, and **7** confirm the at least partial existence of the complexes in MeCN solution, signals due to $[\text{ZnX}(\text{L})]^+$, $[\text{ZnX}(\text{L})_2]^+$, and $[\text{Zn}(\text{L})_2]^{+2}$ species being always found in our conditions. The poor solubility of the cadmium species in MeCN prevents obtaining of ESI MS spectra, whereas in the case of Hg complexes the most

(25) Bailey, R. A.; Kozak, S. L.; Michelsen, T. W.; Mills, W. N. *Coord. Chem. Rev.* **1971**, *6*, 407.

(26) Mitchell, P. C. H.; Williams, R. J. P. *J. Chem. Soc.* **1960**, 1912.

(27) Lorenzotti, A.; Bonati, F.; Cingolani, A.; Leonesi, D.; Pettinari, C. *Gazz. Chim. Ital.* **1991**, *121*, 551.

(28) Pettinari, C.; Marchetti, F.; Lorenzotti, A.; Gioia Lobbia, G.; Leonesi, D.; Cingolani, A. *Gazz. Chim. Ital.* **1994**, *124*, 51.

(29) Bovio, B.; Cingolani, A.; Pettinari, C.; Gioia Lobbia, G.; Bonati, F. *Z. Anorg. Allg. Chem.* **1991**, *602*, 169.

(30) Pettinari, C.; Santini, C.; Leonesi, D.; Cecchi, P. *Polyhedron* **1994**, *13*, 1553.

(31) Pettinari, C.; Gioia Lobbia, G.; Lorenzotti, A.; Cingolani, A. *Polyhedron* **1995**, *14*, 793.

(20) Reedijk, J. *Rec. Trav. Chim.* **1969**, *88*, 1451.

(21) Mesubi, M. A.; Anumba, F. O. *Trans. Met. Chim.* **1985**, *10*, 5.

(22) Lever, A. B. P.; Mantovani, E.; Ramaswamy, B. S. *Can. J. Chem.* **1971**, *49*, 1957.

(23) Lott, A. L. *Inorg. Chem.* **1974**, *13*, 667–670.

(24) Curtis, N. F.; Curtis, I. M. *Inorg. Chem.* **1965**, *4*, 804–809.

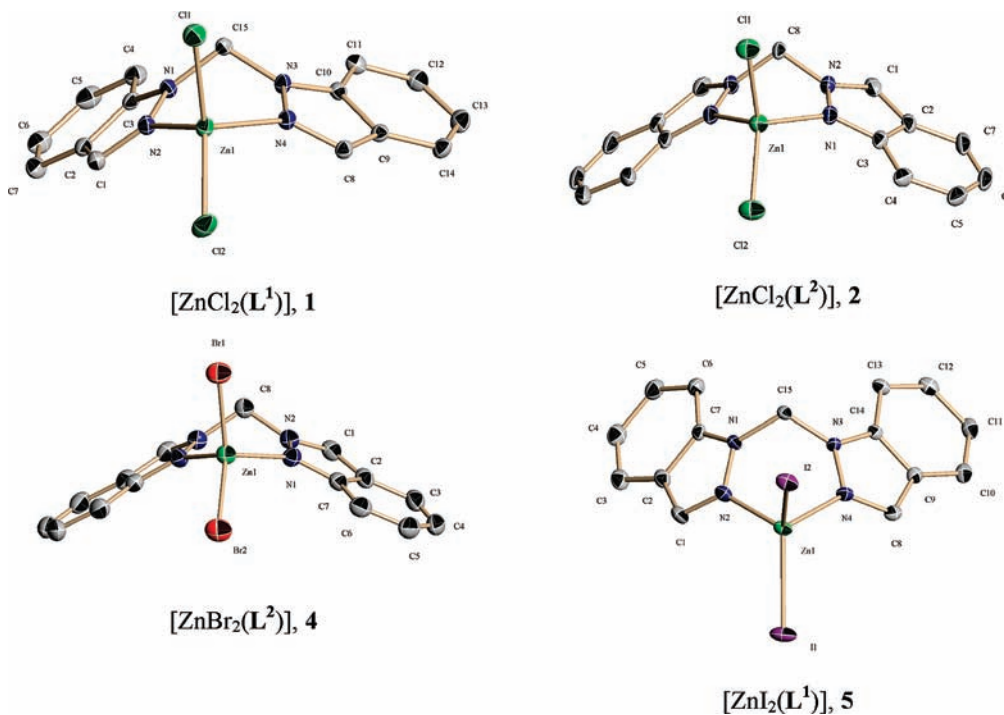
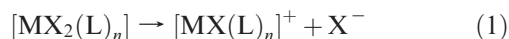


Figure 1. Molecular views of compounds **1**, **2**, **4**, and **5** with displacement ellipsoids drawn at the 50% probability level (except for **5** at 30%). All H atoms are omitted for clarity.

evident signals are ascribed to solvated species such as $[\text{HgX}(\text{solv})]^+$.

The chloride adducts **1–2**, **11**, and **15–16** are not electrolytes in DMSO solutions, thus ruling out self-ionization or displacement reaction of the anion by the solvent as those represented in the eqs 1 and 2:



On the other hand the Λ_m values found for the bromide and iodide complexes **3–6** suggest the occurrence of ionization processes as (1) and (2), the iodide species being more ionized than bromides.³²

The nitrate derivatives **7**, **8**, and **10** seem to be partially dissociated in DMSO and MeCN, whereas the derivative **9** behaves as a 1:2 electrolyte, Λ_m being in the range 70–90 S cm² mol⁻¹.³²

The thermal behavior of selected complexes has been studied by TGA between 25 and 500 °C. The TG curves showed most complexes studied to be non-solvated. The most stable to decomposition proved to be the chloride species **1**, **2**, **12**, **14**, and **15**, the zinc and cadmium species **1** and **12** being the more stable with respect to mercury derivatives, the former starting to decompose at about 320 and 300 °C, compared to about 200–210 °C for mercury species.

Crystallography. Crystal Structure of 1 and 5. Both compounds **1** and **5** crystallize in the monoclinic space group $P2_1/n$. The asymmetric unit for both compounds contains in the same way one $[\text{ZnX}_2(\text{L}^1)]$ molecule where X = Cl for **1** and X = I for **5** (Figure 1). The Zn center in both crystal structures **1** and **5** is tetrahedrally coordinated by two nitrogen atoms from one L^1 ligand and two halide

atoms. In addition the Zn–N and Zn–X bond lengths for **1** and **5** are shown in Table 3, and they are comparable to other similar $\text{ZnX}_2(\text{azol})$ complexes.^{33,34} The angles X(1)–Zn(1)–X(2) = 124.550(18)° and 120.845(19)° for **1** and **5** respectively, show the largest deviation from idealized tetrahedral angle, whereas the smallest deviations are presented by N(4)–Zn(1)–N(2) = 90.37(4)° and 89.32(12)° for **1** and **5** respectively. The adjacent $[\text{ZnX}_2(\text{L}^1)]$ molecules are stacked in a face-to-face fashion with separations between the closest indazolyl ring centroids of 3.463 Å and 3.853 Å for **1** and **5**, respectively, indicative of the existence of significant intermolecular π – π interactions.

Crystal Structure of 2 and 4. Compound **2** crystallizes in the monoclinic space group $P2_1/m$ while compound **4** crystallizes in the orthorhombic space group $Pnma$; however, in both crystals the asymmetric unit contains one-half of a $[\text{ZnX}_2(\text{L}^2)]$ molecule (Figure 1) where X = Cl for **2** and X = Br for **4**. This is because both molecules **2** and **4** have a crystallographic mirror plane passing through the Zn1, X1, X2, and C8 atoms. The Zn center in both **2** and **4** is tetrahedrally coordinated by two nitrogen atoms from one L^2 ligand and two halide atoms. The Zn–N and the Zn–X bond lengths are shown in Table 3, and they are comparable to other $[\text{ZnX}_2(\text{azol})]$ complexes.³³ The angles X(1)–Zn(1)–X(2) = 121.556(15)° and 120.32(3)° for **2** and **4**, respectively, show the largest deviation from idealized tetrahedral angle, and the smallest deviations are shown by N(1)#1–Zn(1)–N(1) = 90.8(4)° and 91.40(15)° (#1 $x, -y + 1/2, z$) for **2** and **4**, respectively. The adjacent $[\text{ZnX}_2(\text{L}^2)]$ molecules are stacked in a face-to-face fashion

(33) Bond length statistics were analyzed using the program Vista from a ConQuest search of the Cambridge Structural Database (CSD). CSD Version 5.31, Conquest 1.12 & Vista. <http://www.ccdc.cam.ac.uk/> (accessed July 2010).

(34) Caverio, E.; Uriel, S.; Romero, P.; Serrano, J. L.; Gimenez, R. *J. Am. Chem. Soc.* **2007**, *129*, 11608.

(32) Geary, W. J. *Coord. Chem. Rev.* **1971**, *7*, 81.

with separation of 3.961 Å and 3.721 Å for **2** and **4**, respectively, between the closest phenyl ring centroids of the antiparallel indazolyl moieties, thus indicating the existence of slighter intermolecular π - π interactions than those for **1** and **5**.

Crystal Structure of 7, 8. Although the reaction of **L**¹ with Zn(NO₃)₂·6H₂O was dependent on the ligand to metal ratio employed such as stated above, the crystals obtained from this reaction always gave the same cell metric and Laue symmetry, once the cell parameters were determined, independent of the ligand to metal ratio employed. Compounds **7**, **8** crystallize in the orthorhombic space group *Pbca*, and their asymmetric unit contains two different zinc nitrate structures: one [Zn(NO₃)₂(**L**¹)], **7** molecule and one-half of a [Zn(NO₃)₂(**L**¹)₂], **8** molecule (Figure 2). The Zn nitrate complex **7** appears pseudooctahedral six-coordinated by two nitrogen atoms from one **L**¹ ligand and four oxygen atoms from two bidentate nitrate anions. Whereas the Zn center of **8** appears octahedrally six-coordinated by four nitrogen atoms belonging to two **L**¹ ligands and two oxygen atoms from two unidentate nitrate anions. The Zn–N bond lengths and the Zn–O bond lengths are shown in Table 3, and they are comparable to those of other [Zn(NO₃)₂(azole)] complexes.^{33,35} The adjacent **7** and **8** molecules are stacked between them in a face-to-face fashion, with separation from 3.856 to 3.930 Å between the centroids of the two neighbors indazolyl rings (pyrazolyl-phenyl, phenyl-pyrazolyl rings) belonging one to **7** and other one to **8**, indicating also the existence of intermolecular π - π interactions.

Crystal Structure of 10. Compound **10** crystallizes in the monoclinic space group *C2/c*, and its asymmetric unit contains one zinc nitrate salt, in such a way that it presents one cationic [Zn(NO₃)(**L**²)]⁺ molecule (Figure 2), one free [NO₃][−], and one free half water of crystallization. The Zn cationic molecule of **10** appears pseudooctahedral six-coordinated by four nitrogen atoms from two **L**² ligands and two oxygen atoms from one bidentate nitrate anion. The Zn–N bond lengths and the Zn–O bond lengths are shown in Table 3, and they are comparable to **7** and **8** zinc nitrate complexes. The adjacent cationic [Zn(NO₃)(**L**²)]⁺ molecules are stacked in an offset face-to-face and in a edge-to-face fashion with separations of 3.472 Å and 2.923 Å, respectively, between the centroid of one phenyl-pyrazolyl ring and the hydrogen atom of the neighbor phenyl-pyrazolyl ring, indicating the existence of the significant intermolecular π -stacking interactions.

Crystal structure of 11. Compound **11** crystallizes in the triclinic space group *P1*, and its asymmetric unit contains one [CdCl₂(**L**²)₂] molecule (Figure 3). The cadmium center of **11** is octahedral coordinated by four nitrogen atoms from two **L**² ligands and two chloride atoms. The Cd–N bond lengths and the Cd–Cl bond lengths are shown in Table 4, and they are comparable to those of [CdCl₂(azole)] complexes.³³ One of the major differences between ZnCl₂(**L**²)_{*n*} **2** (*n* = 1) and CdCl₂(**L**²)_{*n*} **11** (*n* = 2) adducts is the much stronger tendency for the latter to expand its coordination sphere and adopt an octahedral over tetrahedral geometry. The adjacent [CdCl₂(**L**²)₂] molecules are stacked in a face-to-face fashion with separation of 3.821 Å between

Table 3. List of Selected Bond Distances [Å] and Angles [deg] for Zn(II) Compounds **1**, **2**, **4**, **5**, **7**, **8**, and **10**

Compound 1			
Zn(1)–N(2)	2.0716(11)	N(4)–Zn(1)–N(2)	90.37(4)
Zn(1)–N(4)	2.0615(11)	Cl(2)–Zn(1)–Cl(1)	124.550(18)
Zn(1)–Cl(1)	2.2135(4)	Zn(1)–Cl(2)	2.1910(4)
Compound 2 ^a			
Zn(1)–N(1)	2.067(7)	N(1)#1–Zn(1)–N(1)	90.8(4)
Zn(1)–Cl(1)	2.227(4)	Cl(2)–Zn(1)–Cl(1)	121.56(15)
Zn(1)–Cl(2)	2.214(4)		
Compound 4 ^b			
Zn(1)–N(1)	2.049(3)	N(1)–Zn(1)–N(1)#1	91.40(15)
Zn(1)–Br(2)	2.3434(7)	Br(2)–Zn(1)–Br(1)	120.32(3)
Zn(1)–Br(1)	2.3560(8)		
Compound 5			
Zn(1)–N(4)	2.066(3)	N(4)–Zn(1)–N(2)	89.32(12)
Zn(1)–N(2)	2.080(3)	I(1)–Zn(1)–I(2)	120.845(19)
I(1)–Zn(1)	2.5243(5)	I(2)–Zn(1)	2.5416(5)
Compound 7			
Zn(1)–N(2)	2.058(2)	N(2)–Zn(1)–N(4)	93.15(8)
Zn(1)–N(4)	2.069(2)	O(2)–Zn(1)–O(1)	58.03(9)
Zn(1)–O(2)	2.076(2)	O(4)–Zn(1)–O(5)	59.53(9)
Zn(1)–O(4)	2.154(2)	Zn(1)–O(1)	2.314(3)
Zn(1)–O(5)	2.184(2)		
Compound 8			
Zn(2)–N(8)	2.1510(19)	N(8)–Zn(2)–O(7)	88.43(7)
Zn(2)–O(7)	2.1640(16)	N(8)–Zn(2)–N(10)	90.67(7)
Zn(2)–N(10)	2.1740(18)	O(7)–Zn(2)–N(10)	93.45(7)
N(11)–O(7)–Zn(2)	124.27(14)		
Compound 10			
N(1)–Zn(1)	2.1423(15)	Zn(1)–O(2)	2.2077(14)
Zn(1)–N(3)	2.0816(15)	Zn(1)–O(1)	2.2615(14)
Zn(1)–N(7)	2.1063(15)	N(3)–Zn(1)–N(1)	87.14(6)
Zn(1)–N(5)	2.1227(15)	N(7)–Zn(1)–N(5)	87.15(5)
		O(2)–Zn(1)–O(1)	57.82(5)

^aSymmetry transformations used to generate equivalent atoms: #1 *x*, *−y* + 1/2, *z*. ^bSymmetry transformations used to generate equivalent atoms: #1 *x*, *−y* + 1/2, *z*.

the centroids of the one phenyl ring from an indazolyl moieties with one pyrazol ring from a neighbor indazolyl moieties, indicating the existence of intermolecular π - π aromatic interactions.

Crystal Structure of 12. Compound **12** crystallizes in the monoclinic space group *C2/c* and exhibits polymeric structure in the solid state. A low temperature X-ray crystallographic study shows that the structure consists of an infinite linear chain of the asymmetric unit [Cd(μ -Br)₂(**L**¹)]. This motif is repeated indefinitely along the crystallographic *c* axis, alternating successively a crystallographic center of symmetry and a crystallographic 2-fold axis, **12** showing the polymeric structure [Cd(μ -Br)₂(**L**¹)]_{*n*}. Thus, the cadmium atoms, bridging by two bromine atoms among themselves, Cd₂(μ -Br)₂ cores, extend non-linearly along the crystallographic *c* axis by alternating successively a center of symmetry and a 2-fold axis forming a main polymer chain. The 2-fold axes and the centers of symmetry are placed in the center of the Cd₂(μ -Br)₂ cores, the first ones perpendicular to the plane of the cores and the last ones forming an aligned straight line with the crystallographic *c* axis. Considered independently each cadmium atom shows a

(35) Cheng, M.-L.; Cao, X.-Q.; Wang, C.-L.; Li, H.-X.; Lang, J.-P. *Wuji Huaxue Xuebao (Chin. J. Inorg. Chem.)* **2006**, *22*, 1222.

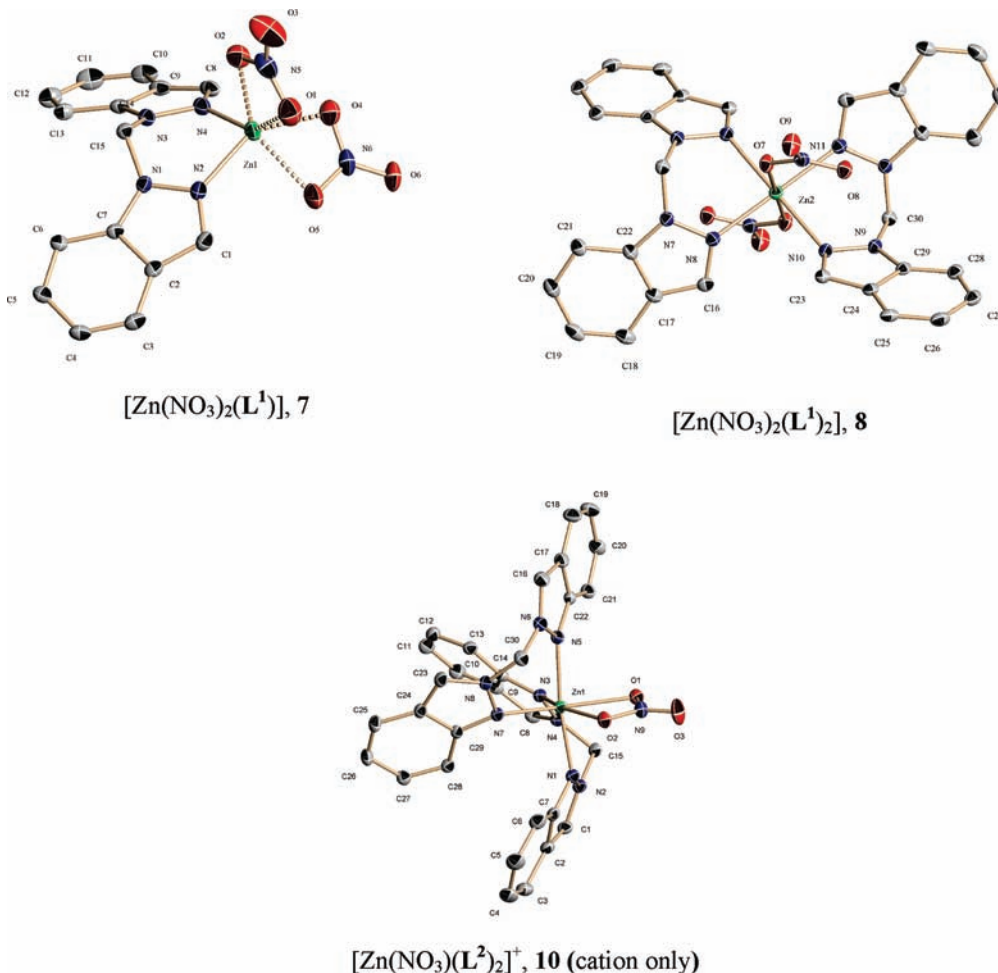


Figure 2. Molecular views of compounds **7**, **8**, and **10** (cation only for clarity). The displacement ellipsoids are drawn at the 30% probability level. All H atoms are omitted for clarity.

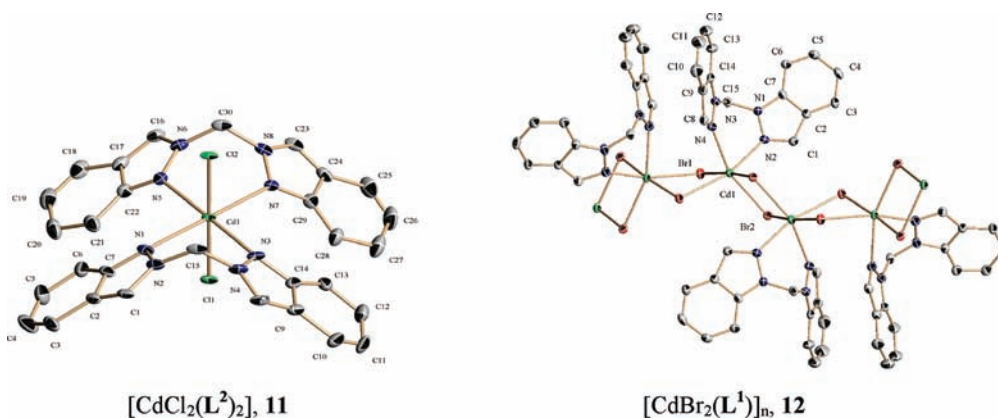


Figure 3. Molecular views of compounds **11** and **12**. Displacement ellipsoids have been drawn at the 30 and 50% probability level, respectively, and all H atoms have been omitted for clarity.

slightly distorted octahedral geometry, coordinated by two nitrogen atoms from the L^1 ligand and four bridging bromine atoms. The Cd–N bond lengths and the Cd–Br bridge bond lengths are shown in Table 4, and they are comparable to analogous two bromine bridged cadmium(II)

dinuclear complexes.³⁶ In this polymeric complex **12**, pairs of symmetrically intramolecular indazolyl moieties by a 2-fold axis, belonging to the same polymer chain, are stacked in a face-to-face fashion with a separation of 3.784 Å. Neighbor polymeric chains are linked to each other by means of intermolecular π – π aromatic interactions of indazolyl moieties, stacked in a face-to-face fashion with separation of 3.490 Å, between the centroids of

(36) Matsunaga, Y.; Fujisawa, K.; Amir, N.; Miyashita, Y.; Okamoto, K. *Appl. Organomet. Chem.* **2005**, *19*, 778.

Table 4. List of Selected Bond Distances [Å] and Angles [deg] for Cd(II) and Hg(II) Compounds **11**, **12**, **14**, **15**, and **19**

Compound 11			
Cd(1)–N(3)	2.354(16)	Cd(1)–Cl(2)	2.527(4)
Cd(1)–N(1)	2.398(15)	Cd(1)–Cl(1)	2.547(5)
Cd(1)–N(7)	2.430(13)	N(3)–Cd(1)–N(1)	81.6(6)
Cd(1)–N(5)	2.451(15)	N(7)–Cd(1)–N(5)	79.8(5)
		Cl(2)–Cd(1)–Cl(1)	179.7(2)
Compound 12 ^a			
Cd(1)–N(2)	2.400(4)	Cd(1)–Br(2)#2	2.8484(5)
Cd(1)–N(4)	2.431(4)	N(2)–Cd(1)–N(4)	78.10(13)
Cd(1)–Br(2)	2.6937(5)	Cd(1)#1–Br(1)–Cd(1)	92.829(15)
Cd(1)–Br(1)#1	2.7402(5)	Cd(1)–Br(2)–Cd(1)#2	95.367(15)
Cd(1)–Br(1)	2.7745(5)		
Compound 14			
Hg(1)–Cl(1)	2.343(2)	Hg(1)–N(4)	2.563(7)
Hg(1)–Cl(2)	2.350(2)	Cl(1)–Hg(1)–Cl(2)	160.96(8)
Hg(1)–N(2)	2.524(7)	Cl(3)–Hg(2)–Cl(4)	167.42(8)
N(2)–Hg(1)–N(4)	76.3(2)	N(8)–Hg(2)–N(6)	75.2(2)
Compound 15 ^b			
Hg(1)–Cl(1)	2.394(8)	N(1)–Hg(1)–N(3)#1	76.3(3)
Hg(1)–Cl(2)	2.431(8)	N(1)–Hg(1)–N(3)	103.5(3)
Hg(1)–N(1)	2.618(9)	Cl(1)–Hg(1)–Cl(2)	180.000(2)
Hg(1)–N(3)	2.622(9)		
Compound 19			
Hg(1)–N(3)	2.396(3)	S(1)–Hg(1)–S(2)	144.65(4)
Hg(1)–S(1)	2.4140(12)	N(3)–Hg(1)–N(1)	77.48(12)
Hg(1)–S(2)	2.4148(12)		
Hg(1)–N(1)	2.467(4)		

^a Symmetry transformations used to generate equivalent atoms: #1 $-x, y, -z+3/2$; #2 $-x, -y, -z+1$. ^b Symmetry transformations used to generate equivalent atoms: #1 $-x, y, -z$.

the two phenyl rings from antiparallel indazolyl moieties belonging to neighboring chains, indicating the existence of significant intermolecular π – π aromatic interactions.

Crystal Structure of 14. Compound **14** crystallizes in the triclinic space $P\bar{1}$, and the asymmetric unit contains two symmetrically independent but equivalent $[\text{HgCl}_2(\text{L}^1)]$ molecules including secondary Hg---Cl interactions between both (Figure 4), indicative of **14** would be a “dinuclear-like” complex as $[\text{Hg}(\mu\text{-Cl})\text{Cl}(\text{L}^1)]_2$. Hence, the Hg(II) centers in the mononuclear complexes **14** are found to have a severely tetrahedrally distorted geometry, and it is better described as a slightly distorted trigonal-bipyramidal geometry, pentacoordinated by two nitrogen atoms from one L^1 ligand, one terminal chloride atom, and two differently bridging chloride atoms, that is, one primary Hg–Cl bond and one secondary Hg---Cl interaction. The Hg–N bond lengths and the primary Hg–Cl bond lengths are shown in Table 4, and they are comparable to other $[\text{HgCl}_2(\text{azole})]$ complexes.^{33,37} The angles Cl(1)–Hg(1)–Cl(2) = 160.96(8)° and Cl(3)–Hg(2)–Cl(4) = 167.42(8)°, respectively, show severe deviations from idealized tetrahedral angles, whereas the smallest deviations are shown by N(2)–Hg(1)–N(4) = 76.3(2)° and N(8)–Hg(2)–N(6) = 75.2(2)°, respectively. The secondary Hg---Cl interactions between the two independent $[\text{HgCl}_2(\text{L}^1)]$ complexes are Hg(1)–Cl(2)---Hg(2) = 3.116 Å and Hg(2)–Cl(4)---Hg(1) = 3.389 Å,

respectively, longer than the primary Hg–Cl bond lengths. These secondary Hg---Cl interactions represent mainly dipole–dipole forces. According to simple bond-distance versus bond-valence models, their strength is about 5–10% that of a Hg–Cl single bond.³⁸ The adjacent $[\text{HgCl}_2(\text{L}^1)]$ molecules are stacked in a offset face-to-face and in a edge-to-face fashion with separations of 3.507 Å and 3.686 Å, respectively, between the centroid of one phenyl-pyrazolyl ring and the hydrogen atom of the neighbor phenyl-pyrazolyl ring, indicating also the existence of the significant intermolecular aromatic interactions.

Crystal Structure of 15. Compound **15** crystallizes in the monoclinic space group $C2$, and its asymmetric unit contains two-half of equivalent but symmetrically independent $[\text{HgCl}_2(\text{L}^2)]_2$ molecules. As shown in Figure 4 both structures contain a crystallographic 2-fold axis passing through the mercury metal and both chlorine atoms. Therefore, the mercury center for **15** is octahedral coordinated by four nitrogen atoms from two L^2 ligands and two chloride atoms. The Hg–N bond lengths and the Hg–Cl bond lengths are shown in Table 4, and they are comparable to those of other $[\text{HgCl}_2(\text{azol})]$ complexes. The solid crystalline structure of **15** is formed by parallel and displaced chains of $[\text{HgCl}_2(\text{L}^2)]_2$ complexes along the crystallographic axis a , stacked in a face-to-face fashion with separation of 3.688 Å between the centroids of the one phenyl ring from an indazolyl moiety with one pyrazol ring from a neighbor parallel indazolyl moiety, indicating the existence of intermolecular π – π aromatic interactions.

Crystal Structure of 19. Compound **19** crystallizes in the monoclinic space group $P2_1/n$, and its asymmetric unit contains one $[\text{Hg}(\text{SCN})(\text{L}^2)]$ molecule (Figure 4), including secondary Hg---S interactions with a neighboring molecule symmetrically related by an inversion center. These secondary interactions give the appearance that **19** would be a “dinuclear-like” complex as $[\text{Hg}(\mu\text{-SCN})(\text{SCN})(\text{L}^2)]_2$. Hence, similar to the **14** complex, the Hg(II) center in the mononuclear complex **19** is found to have a severely tetrahedrally distorted geometry, and it is better described also as a slightly distorted trigonal-bipyramidal geometry, pentacoordinated by two nitrogen atoms from one L^2 ligand, one terminal sulfocyanide anion, and two differently bridging sulfocyanide anions, that is, one primary Hg–SCN bond and one secondary Hg---SCN interaction. The Hg–N bond lengths and the primary Hg–SCN bond lengths are shown in Table 4, and they are comparable to those of other $[\text{Hg}(\text{SCN})_2(\text{azole})]$ complexes.³³ The angle S(1)–Hg(1)–S(2) = 144.65(4)° shows severe deviation from an idealized tetrahedral angle, whereas the smallest deviation is N(3)–Hg(1)–N(1) = 77.48(2)°. The secondary Hg---SCN interaction between the two symmetrically dependent $[\text{Hg}(\text{SCN})_2(\text{L}^2)]$ complexes is 3.544 Å, higher than the primary Hg–SCN bond length (Table 4). These secondary Hg---SCN interactions represent mainly dipole–dipole forces. According to simple bond-distance versus bond-valence models, their strength is about 5–10% that of a Hg–SCN single bond.³⁴ The adjacent $[\text{Hg}(\mu\text{-SCN})(\text{SCN})(\text{L}^2)]_2$ molecules are stacked in a offset face-to-face and in a edge-to-face fashion with separations of 4.008 Å and 4.212 Å, respectively, between the centroid of one phenyl-pyrazolyl ring and the hydrogen atom of the

(37) (a) Del Hierro, I.; Sierra, I.; Perez-Quintanilla, D.; Carrillo-Hermosilla, F.; Lopez-Solera, I.; Fajardo, M. *Inorg. Chim. Acta* **2003**, *355*, 347. (b) Marsh, R. E. *Acta Crystallogr., Sect. B: Struct. Sci.* **2005**, *61*, 359.

(38) Brese, N. E.; O’Keeffe, M. *Acta Crystallogr.* **1991**, *B47*, 192.

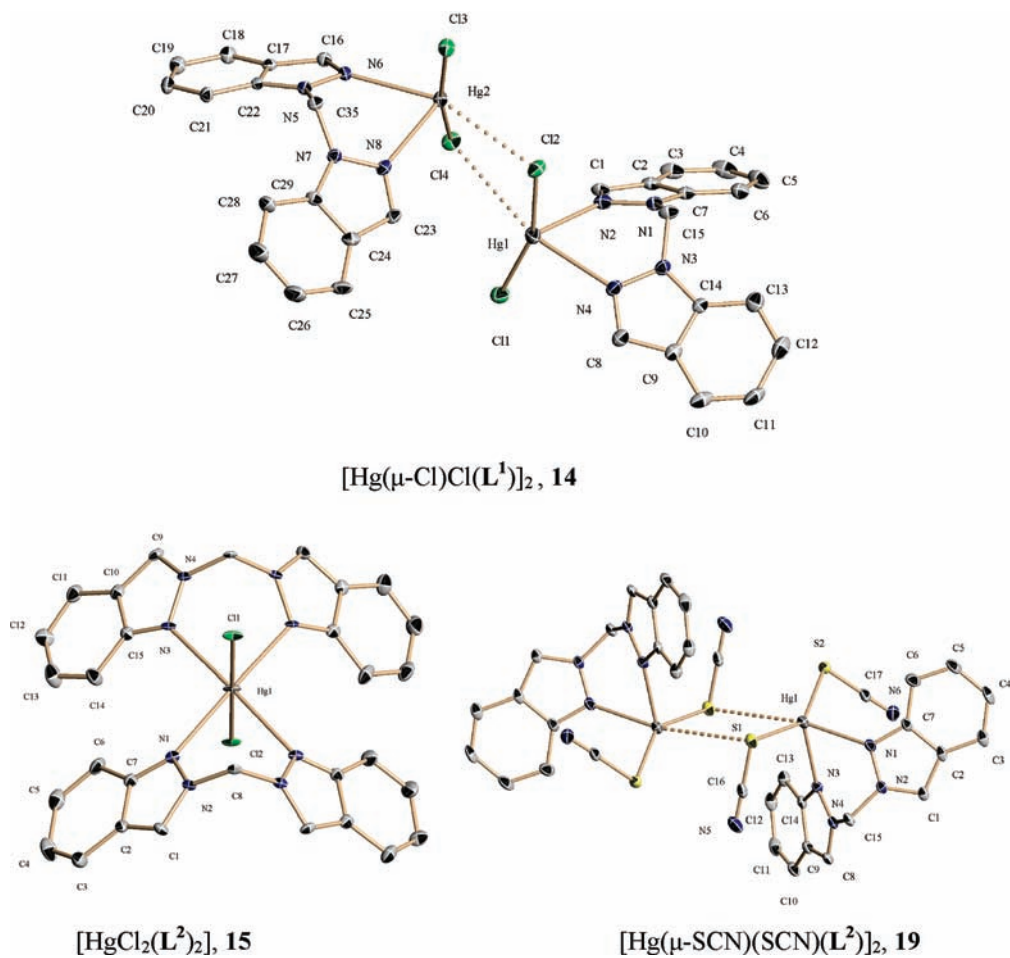


Figure 4. Molecular views of compounds **14**, **15**, and **19**. Displacement ellipsoids are drawn at the 30% probability level (except for **19** at 50%), and all H atoms are omitted for clarity.

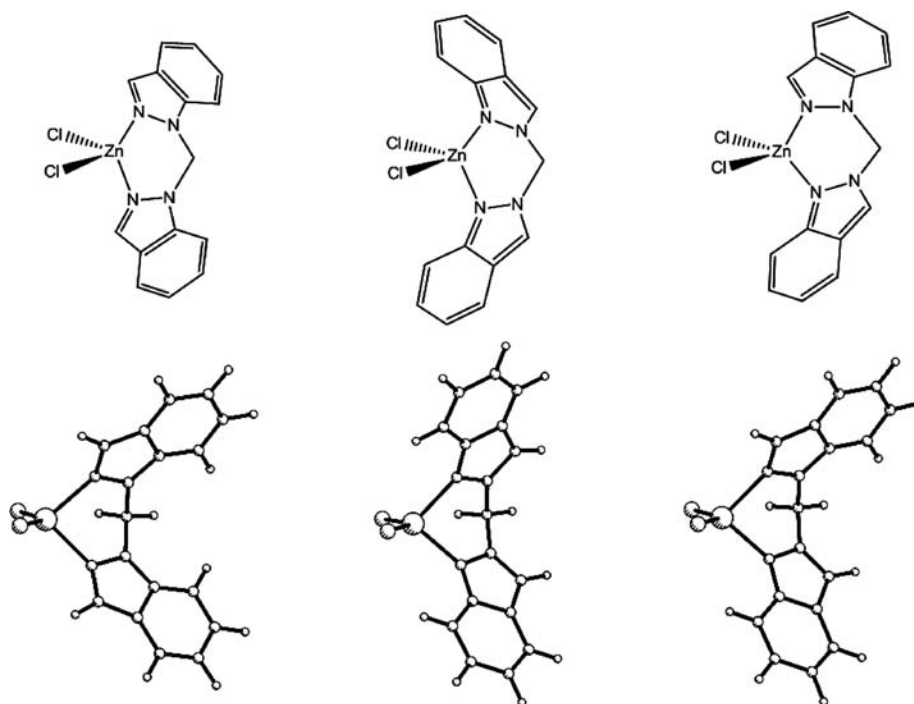


Figure 5. Optimized structures of the compounds **1c**, **2c**, and **Zn $\alpha\beta$** .

neighbor phenyl-pyrazolyl ring, indicating also the existence of the significant intermolecular aromatic interactions.

Theoretical Calculations of ZnCl₂(L) Compounds. DFT calculations of compounds **1**, **2** and of the complex containing the $\alpha\beta$ isomer of di(indazolyl)methane have been performed at the B3LYP level. The resulting optimized structures, **1c**, **2c**, and **Zn $\alpha\beta$** , are shown in Figure 5. All of them are stationary points on the potential energy surface (PES) as confirmed by the calculations of the frequencies.

The reproducibility of the experimental geometry is satisfactory and a comparison of selected computed and experimental geometric parameters is included in the Supporting Information, Table S3. A small but significant difference was found concerning the puckering of the boat conformation of the Zn-di(indazolyl)methane metallacycle. For instance, comparing **2** and **2c**, the non-bonding distance between one chloro ligand and one hydrogen atom of the CH₂ group is 2.996 Å (**2**), while the computed value is 2.555 Å (**2c**). This is due to the intermolecular Cl \cdots H–C interactions found in the crystal and obviously not considered in the calculations (see Supporting Information, Figure S2). The localization of the π system of the rings in the di(indazolyl)methane ligand is well described by calculations (Supporting Information, Figure S3) and compares well with that experimentally found in compounds **1** and **2** and also in the free ligands.^{8b} From an energetic point of view, the compound **1c**, with the $\alpha\alpha$ isomer of di(indazolyl)methane, is the most stable. The complex containing the $\alpha\beta$ isomer of di(indazolyl)methane, namely, **Zn $\alpha\beta$** , is close in energy (3.3 kcal mol⁻¹), while compound **2c**, with the $\beta\beta$ isomer, is higher in energy by 7.7 kcal mol⁻¹. This fact agrees with the energy differences previously computed for the free ligands.^{8b}

Conclusions

Our work aimed at the preparation of novel Groups 12 metal adducts containing two indazolyl-based regioisomeric ligands, for the first time separated and independently used to coordinate metals. One major focus was the synthesis of analogous adducts of both regioisomers to allow a full comparison of their structural and spectral features.

NMR, IR, and ESI MS spectroscopies and mainly X-ray studies allowed to confirm the stoichiometries and the N,N chelating coordination modes of the new indazolylmethane ligands in their metal complexes. It is noteworthy that in the case of zinc(II) halide complexes both ligands behave in a similar manner, yielding always 1:1 adducts having a tetrahedral geometry, independently on the reaction condition employed, whereas in the case of zinc(II) nitrate derivatives, also in the presence of a similar composition, the greater steric hindrance of the ligand **L**² provokes a displacement of a NO₃ group from the Zn coordination sphere.

We have demonstrated that **L**¹ and **L**² interact with nitrate salts yielding adducts with different stoichiometries simply upon changing the reaction conditions. This behavior is new for the bis(pyrazolyl)alkane ligands family, as reported in Table 6 of ref 30. Similarly **L**² reacts with CdCl₂ affording a 2:1 adduct, a stoichiometry not previously reported with R₂C(pz)₂ ligands.^{30,31} Because indazole is less basic than pyrazole,³⁹ the 2:1 ligand to metal ratio is likely a consequence of the higher steric hindrance of **L**² with respect to the other members of the ligand family. On the other hand when the less sterically hindered **L**¹ reacts with CdBr₂ no full disruption of the Cd–Br–Cd chains occurs, **L**¹ being coordinated in the chelating form and able to yield a 1:1 polymeric adduct. Finally, the reaction of **L**¹ and **L**² with HgX₂ gave both 1:1 and 2:1 adducts. The 2:1 ratio has not previously reported for mercury derivatives of R₂C(pz)₂^{30,31} suggesting that a fine-tuning of steric and electronic properties of the R₂C(pz)₂ family can provide different stoichiometry for the adducts.

Acknowledgment. Financial support from University of Camerino, Valle-Esina Spa, the bilateral italian-spanish integrated action (HI2006-0125), the Junta de Andalucía (Projects P09-FQM-4826 and P07-FQM-2474) and CSIC (PIF08-017-1) is gratefully acknowledged.

Supporting Information Available: X-ray crystallographic files in CIF format for the X-ray structure determination of **1**, **2**, **4**, **5**, **7**, **8**, **10**, **11**, **12**, **14**, **15**, and **19**. Selected spectroscopic data, comparison of selected structural parameters and coordinates of the optimized structures. This material is available free of charge via the Internet at <http://pubs.acs.org>.

(39) Eicher, T.; Hauptmann, S. *The Chemistry of Heterocycles*; Wiley-VCH: Weinheim, 2003.